Effects of NO_x and SO_2 on the Secondary Organic Aerosol Formation from Photooxidation of α-pinene and Limonene

Defeng Zhao[1], Sebastian H. Schmitt[1], Mingjin Wang[1, 2], Ismail-Hakki Acir[1, a], Ralf Tillmann[1], Zhaofeng Tan[1, 2], Anna Novelli[1], Hendrik Fuchs[1], Iida Pullinen[1, b], Robert Wegener[1], Franz Rohrer[1], Jürgen Wildt[1], Astrid Kiendler-Scharr[1], Andreas Wahner[1], Thomas F. Mentel[1]

[1] Institute of Energy and Climate Research, IEK-8: Troposphere, Forschungszentrum Jülich, Jülich, 52425, Germany

[2] College of Environmental Science and Engineering, Peking University, Beijing, 100871, China

[a]Now at: Institute of Nutrition and Food Sciences, University of Bonn, Bonn, 53115, Germany; [b]Now at: Department of Applied Physics, University of Eastern Finland, Kuopio, 7021, Finland.

Correspondence to: Th. F. Mentel (t.mentel@fz-juelich.de)

Abstract

Anthropogenic emissions such as NO_x and SO_2 influence the biogenic secondary organic aerosol (SOA) formation, but detailed mechanisms and effects are still elusive. We studied the effects of NO_x and SO_2 on the SOA formation from the photooxidation of α-pinene and limonene at ambient relevant NO_x and SO_2 concentrations (NO_x: < 1 ppb to 20 ppb, SO_2: <0.05 ppb to 15 ppb). In these experiments, monoterpene oxidation was dominated by OH oxidation. We found that SO_2 induced nucleation and enhanced SOA mass formation. NO_x strongly suppressed not only new particle formation but also SOA mass yield. However, in the presence of SO_2 which induced high number concentration of particles after oxidation to H_2SO_4, the suppression of the mass yield of SOA by NO_x was completely or partly compensated. This indicates that the suppression of SOA yield by NO_x was largely due to the suppressed new particle formation, leading to a lack of particle surface for the organics to condense on and thus a significant influence of vapor wall loss on SOA mass yield. By compensating for the suppressing effect on nucleation of NO_x, SO_2 also compensated for the suppressing effect on SOA yield. Aerosol mass spectrometer data show that increasing NO_x enhanced nitrate formation. The majority of the nitrate was organic nitrate (57%-77%), even in low NO_x conditions (<~1 ppb). Organic nitrate contributed 7%-26% of total organics assuming a molecular weight of 200 g/mol. SOA from α-pinene photooxidation at high NO_x had generally lower hydrogen to carbon ratio (H/C), compared to low NO_x. The NO_x dependence of the chemical composition can be attributed to the NO_x dependence of the branching ratio of the RO_2 loss reactions, leading to lower fraction of organic hydroperoxides and higher fractions of organic nitrates at high NO_x. While NO_x suppressed new particle formation and SOA mass formation, SO_2 can compensate for such effects, and the combining effect of SO_2 and NO_x may have important influence on SOA formation affected by interactions of biogenic volatile organic compounds (VOC) with anthropogenic emissions.

1 Introduction

Secondary organic aerosol (SOA) have significant impacts on air quality, human health and climate change (Hallquist et al., 2009; Kanakidou et al., 2005; Jimenez et al., 2009; Zhang et al., 2011). SOA mainly originates from biogenic volatile organic compounds (VOC) emitted by terrestrial vegetation (Hallquist et al., 2009). Once emitted into the atmosphere, biogenic VOC can undergo reactions with atmospheric oxidants including OH, O_3 and NO_3, and form SOA. When an air mass enriched in biogenic VOC is transported over an area with substantial anthropogenic emissions or vice versa, the reaction behavior of VOC and SOA formation can be altered due to the interactions of biogenic VOC with anthropogenic emissions such as NO_x, SO_2, anthropogenic aerosol and anthropogenic VOC. A number of field studies have highlighted the role of the anthropogenic-biogenic interactions in SOA formation (de Gouw et al., 2005; Goldstein et al., 2009; Hoyle et al., 2011; Worton et al., 2011; Glasius et al., 2011; Xu et al., 2015a; Shilling et al., 2012), which can induce an "anthropogenic enhancement" effect on SOA formation.

Among biogenic VOC, monoterpenes are important contributors to biogenic SOA due to their high emission rates, high reactivity, and relative high SOA yield compared to isoprene (Guenther et al., 1995; Guenther et al., 2012; Chung and Seinfeld, 2002; Pandis et al., 1991; Griffin et al., 1999; Hoffmann et al., 1997; Zhao et al., 2015b; Carlton et al., 2009). The anthropogenic modulation of the SOA formation from monoterpene can have important impacts on regional and global biogenic SOA budget (Spracklen et al., 2011). The influence of various anthropogenic pollutants on SOA formation of monoterpene have been investigated by a number of laboratory studies (Sarrafzadeh et al., 2016; Zhao et al., 2016; Flores et al., 2014; Emanuelsson et al., 2013; Eddingsaas et al., 2012a; Offenberg et al., 2009; Kleindienst et al., 2006; Presto et al., 2005; Ng et al., 2007; Zhang et al., 1992; Pandis et al., 1991; Draper et al., 2015; Han et al., 2016). In particular, NO_x and SO_2 have been shown to affect SOA formation from monoterpene.

NO_x changes the fate of RO_2 radical formed in VOC oxidation and therefore can change reaction product distribution and aerosol formation. At low NO_x, RO_2 mainly react with HO_2, forming organic hydroperoxides. At high NO_x, RO_2 mainly react with NO, forming organic nitrate (Hallquist et al., 2009; Ziemann and Atkinson, 2012; Finlayson-Pitts and Pitts Jr., 1999). Some studies found that the SOA yield from α-pinene is higher at lower NO_x concentration for ozonolysis (Presto et al., 2005) and photooxidation (Ng et al., 2007; Eddingsaas et al., 2012a; Han et al., 2016; Stirnweis et al., 2017). The decrease of SOA yield with increasing NO_x was proposed to be due to the formation of more volatile products like organic nitrate under high NO_x conditions (Presto et al., 2005). In contrast, a recent study found that the suppressing effect of NO_x is in large part attributed to the effect of NO_x on OH concentration for the SOA from β-pinene oxidation, and after eliminating the effect of NO_x on OH concentration, SOA yield only varies by 20-30% (Sarrafzadeh et al., 2016). Beside the effect of NO_x on SOA yield, NO_x has been found to suppress the new particle formation from VOC directly emitted by Mediterranean trees (mainly monoterpenes) (Wildt et al., 2014) and β-pinene (Sarrafzadeh et al., 2016), thereby reducing condensational sink present during high NO_x experiments.

Regarding the effect of SO_2, the SOA yield of α-pinene photooxidation was found to increase with SO_2 concentration at high NO_x concentrations (SO_2: 0-252 ppb, NO_x: 242-543 ppb, α-pinene: 178-255 ppb) (Kleindienst et al., 2006) and the increase is attributed to the formation of H_2SO_4 acidic aerosol. Acidity of seed aerosol was also found to enhance particle yield of α-pinene at high NO_x (Offenberg et al. (2009): NO_x 100-120

ppb, α-pinene 69-160 ppb; Han et al. (2016): initial NO ~70 ppb, α-pinene 14-18 ppb). In constrast, Eddingsaas et al. (2012a) found that particle yield increases with aerosol acidity only in "high NO" condition (NO_x 800 ppb, α-pinene: 20-52 ppb), but is independent of the presence of seed aerosol or aerosol acidity in both "high NO_2" condition (NO_x 800 ppb)" and low NO_x (NO_x lower than the detection limit of the NO_x analyzer). Similarly, at low NO_x (initial NO <0.3 ppb, α-pinene ~20 ppb), Han et al. (2016) found that the acidity of seed has no significant effect on SOA yield from α-pinene photooxidation. In addition, SO_2 was found to influence the gas phase oxidation products from α-pinene and β-pinene photooxidation, which is possibly due to the change in OH/HO_2 ratio caused by SO_2 oxidation or SO_3 directly reacting with organic molecules (Friedman et al., 2016).

While these studies have provided valuable insights into the effects of NO_x and SO_2 on SOA formation, a number of questions still remain elusive. For example, many studies used very high NO_x and SO_2 concentrations (up to several hundreds of ppb). High NO_x can make the RO_2 radical fate dominated by one single pathway (i.e., RO_2+NO or RO_2+NO_2) to investigate SOA yields and composition under such conditions. Yet, the effects of NO_x and SO_2 at concentration ranges for ambient anthropogenic-biogenic interactions (sub ppb to several tens of ppb for NO_2 and SO_2) have seldom been directly addressed. Moreover, many previous studies on the SOA formation from monoterpene oxidation focus on ozonolysis or do not distinguish OH oxidation and ozonolysis in photooxidation, and only a few studies on OH oxidation have been conducted (Eddingsaas et al., 2012a; Zhao et al., 2015b; McVay et al., 2016; Sarrafzadeh et al., 2016; Henry et al., 2012; Ng et al., 2007). More importantly, studies that investigated the combined effects of NO_x and SO_2 are scarce, although they are often co-emitted from anthropogenic sources. According to previous studies, NO_x can have a suppressing effect on SOA formation while SO_2 can have an enhancing effect. NO_x and SO_2 might have counteracting or synergistic effects in SOA formation in the ambient atmosphere.

In this study, we investigated the effects of NO_x, SO_2 and their combining effects on SOA formation from the photooxidation of α-pinene and limonene. α-pinene and limonene are two important monoterpenes with high emission rates among monoterpenes (Guenther et al., 2012). OH oxidation dominated over ozonolysis in the monoterpene oxidation in this study as determined by measured OH and O_3 concentrations. The relative contributions of RO_2 loss reactions at low NO_x and high NO_x were quantified using measured HO_2, RO_2, and NO concentrations. The effects on new particle formation, SOA yield, and aerosol chemical composition were examined. We used ambient relevant NO_x and SO_2 concentrations so that the results can shed lights on the mechanisms of interactions of biogenic VOC with anthropogenic emissions in the real atmosphere.

2 Experimental

2.1 Experimental setup and instrumentation

The experiments were performed in the SAPHIR chamber (Simulation of Atmospheric PHotochemistry In a large Reaction chamber) at Forschungszentrum Jülich, Germany. The details of the chamber have been described before (Rohrer et al., 2005; Zhao et al., 2015a; Zhao et al., 2015b). Briefly, it is a 270 m³ Teflon chamber using natural sunlight for illumination. It is equipped with a louvre system to switch between light and dark conditions. The physical parameters for chamber running such as temperature and relative humidity were recorded. The solar

irradiation was characterized and the photolysis frequency was derived (Bohn et al., 2005; Bohn and Zilken, 2005).

Gas and particle phase species were characterized using various instruments. OH, HO_2 and RO_2 concentrations were measured using a laser induced fluorescence (LIF) system with details described by Fuchs et al. (2012). OH was formed via HONO photolysis, which was produced from a photolytic process on the Teflon chamber wall (Rohrer et al., 2005). From OH concentration, OH dose, the integral of OH concentration over time, was calculated in order to better compare experiments with different OH levels. For example, experiments at high NO_x in this study generally had higher OH concentrations due to the faster OH production by recycling of $HO_2\bullet$ and $RO_2\bullet$ to OH. The VOC were characterized using a Proton Transfer Reaction Time-of-Flight Mass Spectrometer (PTR-ToF-MS) and Gas Chromatography-Mass spectrometer (GC-MS). NO_x, O_3 and SO_2 concentrations were characterized using a NO_x analyzer (ECO PHYSICS TR480), an O_3 analyzer (ANSYCO, model O341M), and an SO_2 analyzer (Thermo Systems 43i), respectively. O_3 was formed in photochemical reactions since NO_x, even in trace amount (<~1 ppbV), was present in this study. More details of these instrumentation are described before (Zhao et al., 2015b).

The number and size distribution of particles were measured using a condensation particle counter (CPC, TSI, model 3786) and a scanning mobility particle sizer (SMPS, TSI, DMA 3081/CPC 3785). From particle number measurement, the nucleation rate ($J_{2.5}$) was derived from the number concentration of particles larger than 2.5 nm as measured by CPC. Particle chemical composition was measured using a High-Resolution Time-of-Flight Aerosol Mass Spectrometer (HR-ToF-AMS, Aerodyne Research Inc.). From the AMS data, oxygen to carbon ratio (O/C), hydrogen to carbon ratio (H/C), and nitrogen to carbon ratio (N/C) were derived using a method derived in the literature (Aiken et al., 2007; Aiken et al., 2008). An update procedure to determine the elemental composition is reported by Canagaratna et al. (2015), showing the O/C and H/C derived from the method of Aiken et al. (2008) may be underestimated. The H/C and O/C were also derived using the newer approach by Canagaratna et al. (2015) and compared with the data derived from the Aiken et al. (2007) method. The H/C values derived using the Canagaratna et al. (2015) method strongly correlated with the values derived using Aiken et al. (2007) method (Fig. S1) and just increased by 27% as suggested by Canagaratna et al. (2015). Similar results were found for O/C and there was just a difference of 11% in O/C. Since only relative difference in elemental composition of SOA is studied here, only the data derived using Aiken et al. (2007) method are shown as the conclusion was not affected by the methods chosen. The fractional contribution of organics in the signals at m/z=44 and m/z=43 to total organics (f_{44} and f_{43}, respectively) were also derived.

SOA yields were calculated as the ratio of organic aerosol mass formed to the amount of VOC reacted. The mass concentration of organic aerosol was derived using the total aerosol volume concentration measured by SMPS multiplied by the volume fraction of organics with a density of 1 g cm^{-3} to better compare with previous literature. In the experiments with added SO_2, sulfuric acid was formed upon photooxidation and partly neutralized by background ammonia, which was introduced into the chamber mainly due to humidification. The volume fraction of organics was derived based on volume additivity using the mass of organics and ammonium sulfate/ammonium bisulfate from AMS and their respective density (1.32 g cm^{-3} for organic aerosol from one of our previous studies (Flores et al., 2014) and the literature (Ng et al., 2007) and ~1.77 g cm^{-3} for ammonium sulfate/ammonium bisulfate). According to the calculations based on the E-AIM model (Clegg et al., 1998;

4

148   Wexler and Clegg, 2002) (http://www.aim.env.uea.ac.uk/aim/ aim.php), there was no aqueous phase formed at

149   the relative humidity in the experiments of this study. The average RH for the period of monoterpene

150   photooxidation was 28-34% except for one experiment with average RH of 42% RH. The organic aerosol

151   concentration was corrected for the particle wall loss and dilution loss using the method described in Zhao et al.

152   (2015b).

153   2.2   Experimental procedure

154   The SOA formation from α-pinene and limonene photooxidation was investigated at different NO_x and

155   SO_2 levels. Four types of experiments were done: with neither NO_x nor SO_2 added (referred to as "low NO_x, low

156   SO_2"), with only NO_x added (~ 20 ppb NO, referred to as "high NO_x, low SO_2"), with only SO_2 added (~15 ppb,

157   referred to as "low NO_x, high SO_2"), and with both NO_x and SO_2 added (~20 ppb NO and ~15 ppb SO_2, referred

158   to as "high NO_x, high SO_2"). For low NO_x conditions, background NO concentrations were around 0.05-0.2 ppb,

159   and NO was mainly from the background photolytic process of Teflon chamber wall (Rohrer et al., 2005). For

160   low SO_2 conditions, background SO_2 concentrations were below the detection limit of the SO_2 analyzer (0.05

161   ppb). In some experiments, a lower level of SO_2 (2 ppb, referred to as "moderate SO_2") was used to test the effect

162   of SO_2 concentration. An overview of the experiments is shown in Table 1.

163   In a typical experiment, the chamber was humidified to ~75% RH first, and then VOC and NO, if

164   applicable, were added to the chamber. Then the roof was opened to start photooxidation. In the experiments with

165   SO_2, SO_2 was added and the roof was opened to initialize nucleation first and then VOC was added. The particle

166   number concentration caused by SO_2 oxidation typically reached several 10^4 cm^{-3} (see Fig. 2 high SO_2 cases) and

167   after VOC addition, no further nucleation occurred. Adding SO_2 first and initializing nucleation by SO_2

168   photooxidation ensured that enough nucleating particles were present when VOC oxidation started. SO_2

169   concentration decayed slowly in the experiments with SO_2 added and most of the SO_2 was still left (typically

170   around 8 ppb from initial 15 ppb) at the end of an experiment due to its low reactivity with OH. Typical SO_2

171   time series in high SO_2 experiments are shown in Fig S2. The detailed conditions of the experiments are shown in

172   Table S1. The experiments of α-pinene and limonene photooxidation were designed to keep the initial OH

173   reactivity and thus OH loss rate constant so that the OH concentrations of these experiments were more

174   comparable. Therefore, the concentration of limonene was around one-third of the concentration of α-pinene due

175   to the higher OH reactivity of limonene.

176   2.3   Wall loss of organic vapors

177   The loss of organic vapors on chamber walls can influence SOA yield (Kroll et al., 2007; Zhang et al.,

178   2014; Ehn et al., 2014; Sarrafzadeh et al., 2016; McVay et al., 2016; Nah et al., 2016; Matsunaga and Ziemann,

179   2010; Ye et al., 2016; Loza et al., 2010). The wall loss rate of organic vapors in our chamber was estimated by

180   following the decay of organic vapor concentrations after photooxidation was stopped in the experiments with

181   low particle surface area (~5×10^{-8} cm^2 cm^{-3}) and thus low condensational sink on particles. Such method is

182   similar to the method used in previous studies (Ehn et al., 2014; Sarrafzadeh et al., 2016; Krechmer et al., 2016;

183   Zhang et al., 2015). A high-resolution time-of-flight chemical ionization mass spectrometer (HR-ToF-CIMS,

184   Aerodyne Research Inc.) with nitrate ion source ($^{15}NO_3^-$) was used to measure semi/low-volatile organic vapors.

185   The details of the instrument were described in our previous studies (Ehn et al., 2014; Sarrafzadeh et al., 2016).

186   The decay of vapors started from the time when the roof of the chamber was closed. The data were acquired at a

187   time resolution of 4 s. A typical decay of low-volatile organics is shown in Fig. S3 and the first-order wall loss

188   rate was determined to be around 6×10^{-4} s^{-1}.

189   The SOA yield was not directly corrected for the vapor wall loss, but the influence of vapor wall loss on

190   SOA yield was estimated using the method in the study of Sarrafzadeh et al. (2016) and the details of the method

191   are described therein. Briefly, particle surface and chamber walls competed for the vapor loss (condensation) and

192   the condensation on particles led to particle growth. The fraction of organic vapor loss to particles in the sum of

193   the vapor loss to chamber walls and to particles (F_p) was calculated. The vapor loss to chamber walls was derived

194   using the wall loss rate. The vapor loss to particles was derived using particle surface area concentration,

195   molecular velocity and an accommodation coefficient α_p (Sarrafzadeh et al., 2016). $1/F_p$ (f_{corr}) provides the

196   correction factor to obtain the "real" SOA yield. f_{corr} is a function of particle surface area concentration and

197   accommodation coefficient as shown in Fig. S4. Here a range of 0.1-1 for α_p was used, which is generally in line

198   with the ranges of α_p found by Nah et al. (2016) by fitting a vapor-particle dynamic model to experimental data.

199   At a given α_p, the higher particle surface area, the lower f_{corr} and the lower the influence of vapor wall loss are

200   because most vapors condense on particle surface and vice versa. At a given particle surface area, f_{corr} decreases

201   with α_p because at higher α_p a larger fraction of vapors condenses on particles. An average molecular weight of

202   200 g/mol was used to estimate the influence of vapor wall loss. For the aerosol surface area range in most of the

203   experiments in this study (larger than 3×10^{-6} cm^2 cm^{-3}), f_{corr} is less than 1.4 (Fig. S4) and thus the influence of

204   vapor wall loss on SOA yield was relatively small (<~40%). Yet, for the experiments at high NO_x and low SO_2

205   for α-pinene and limonene, the influence of vapor wall loss on SOA can be high due to the low particle surface

206   area, especially at lower α_p. We did not directly correct SOA yield for vapor wall loss because the correction

207   factor (f_{corr}) curve in the low surface area range is very steep and has very large uncertainties (Fig. S4). In

208   addition, α_p also has uncertainties and may depend on the identity of each condensable compounds.

209   **3 Results and discussion**

210   **3.1   Chemical scheme: VOC oxidation pathway and RO_2 fate**

211   In the photooxidation of VOC, OH and O_3 often co-exist and both contribute to VOC oxidation because O_3

212   formation in chamber studies is often unavoidable during photochemical reactions of VOC even in the presence

213   of trace amount of NO_x. In order to study the mechanism of SOA formation, it is helpful to isolate one oxidation

214   pathway from the other. In this study, the reaction rates of OH and ozone with VOC are quantified using

215   measured OH and O_3 concentrations multiplied by rate constants (time series of VOC, OH, and O_3 are shown in

216   Fig. S5). Typical OH and O_3 concentrations in an experiment were around $(1-15)\times10^6$ molecules cm^{-3} and 0-50

217   ppb, respectively, depending on the VOC and NO_x concentrations added. For all the experiment in this study, the

218   VOC loss was dominated by OH oxidation over ozonolysis (see Fig. S6 as an example). The relative importance

219   of the reaction of OH and O_3 with monoterpenes was similar in the low NO_x and high NO_x experiments. At high

220   NO_x, OH was often higher while more O_3 was also produced. The dominant role of OH oxidation in VOC loss

221 makes the chemical scheme simple and it is easier to interpret than cases when both OH oxidation and ozonolysis
222 are important.

223   As mentioned above, RO_2 fate, i.e., the branching of RO_2 loss among different pathways, has an important
224 influence on the product distribution and thus on SOA composition, physicochemical properties, and yields. RO_2
225 can react with NO, HO_2, RO_2, or isomerize. The fate of RO_2 mainly depends on the concentrations of NO, HO_2
226 and RO_2. Here, the loss rates of RO_2 via different pathways were quantified using the measured HO_2, NO and
227 RO_2 concentrations and the rate constants based on the MCM3.3 (Jenkin et al., 1997; Saunders et al., 2003)
228 (*http://mcm.leeds.ac.uk/MCM.*). Measured HO_2 and RO_2 concentrations are shown in Fig. S7 as an example and
229 the relative importance of different RO_2 reaction pathways is compared in Fig. 1, which is similar for both α-
230 pinene and limonene oxidation. In the low NO_x conditions of this study, RO_2+NO dominated the RO_2 loss rate in
231 the beginning of an experiment (Fig. 1a). The trace amount of NO (up to ~0.2 ppbV) was from the photolysis of
232 HONO, which was continuously produced from a photolytic process on chamber walls throughout an experiment
233 (Rohrer et al., 2005). But later in the experiment, RO_2+HO_2 contributed a significant fraction (up to ~40 %) to
234 RO_2 loss because of increasing HO_2 concentration and decreasing NO concentration. In the high NO_x conditions,
235 RO_2+NO overwhelmingly dominated the RO_2 loss rate (Fig. 1b), and with the decrease of NO in an experiment,
236 the total RO_2 loss rate decreased substantially (Fig. 1b). Since the main products of RO_2+HO_2 are organic
237 hydroperoxides, more organic hydroperoxides relative to organic nitrates are expected in the low NO_x conditions
238 here. The loss rate of RO_2+RO_2 was estimated to be ~10^{-4} s^{-1} using a reaction rate constant of 2.5×10^{-13}
239 molecules^{-1} cm^3 s^{-1} (Ziemann and Atkinson, 2012). This contribution is negligible compared to other pathways in
240 this study, although the reaction rate constants of RO_2+RO_2 are highly uncertain and may depend on specific RO_2
241 (Ziemann and Atkinson, 2012). Note that the RO_2 fate in the low and high NO_x conditions quantified here are
242 further used in the discussion below since the information of RO_2 fate is important for data interpretation of
243 experiments conducted at different NO_x levels (Wennberg, 2013).

3.2   Effects of NO_x and SO_2 on new particle formation

245   The effects of NO_x and SO_2 on new particle formation from α-pinene oxidation are shown in Fig. 2a. In
246 low SO_2 conditions, both the total particle number concentration and nucleation rate at high NO_x were lower than
247 those at low NO_x, indicating NO_x suppressed the new particle formation. The suppressing effect of NO_x on new
248 particle formation was in agreement with the findings of Wildt et al. (2014). This suppression is considered to be
249 caused by the increased fraction of RO_2+NO reaction, decreasing the importance of RO_2+RO_2 permutation
250 reactions. RO_2+RO_2 reaction products are believed to be involved in the new particle formation (Wildt et al.,
251 2014; Kirkby et al., 2016) and initial growth of particles by forming higher molecular weight products such as
252 highly oxidized multifunctional molecules (HOM) and their dimers and trimers (Ehn et al., 2014; Kirkby et al.,
253 2016). Although the contribution of RO_2+RO_2 reaction to the total RO_2 loss is negligible, it can contribute a lot to
254 the compounds responsible for nucleation such as dimers and trimers. Generally, organic nitrates and primary
255 organic peroxides (from $RO_2(C_{10})$+HO_2) are not expected to be the main compounds responsible for nucleation
256 since although the volatility of these compounds is low (see below Sect. 3.3.1), it is likely not low enough to
257 nucleate.

In high SO_2 conditions, the nucleation rate and total number concentrations were high, regardless of NO_x levels. The high concentration of particles was attributed to the new particle formation induced by H_2SO_4 alone formed by SO_2 oxidation since the new particle formation occurred before VOC addition. The role of H_2SO_4 in new particle formation has been well studied in previous studies (Berndt et al., 2005; Zhang et al., 2012; Sipila et al., 2010; Kirkby et al., 2011; Almeida et al., 2013).

Similar suppression of new particle formation by NO_x and enhancement of new particle formation by SO_2 photooxidation were found for limonene oxidation (Fig. 2b).

3.3 Effects of NO_x and SO_2 on SOA mass yield

3.3.1 Effect of NO_x

Figure 3a shows SOA yield at different NO_x for α-pinene oxidation. In order to make different experiments more comparable, the SOA yield is plotted as a function of OH dose instead of reaction time. In low SO_2 conditions, NO_x not only suppressed the new particle formation but also suppressed SOA mass yield. Because NO_x suppressed new particle formation, the suppression of the SOA yield could be attributed to the lack of new particles as seed and thus the lack of condensational sink, or to the decrease of condensable organic materials. We further found that when new particle formation was already enhanced by added SO_2, the SOA yield at high NO_x was comparable to that at low NO_x and the difference in SOA yield between high NO_x and low NO_x was much smaller (Fig. 3a). This finding can be attributed to two possible explanations. Firstly, NO_x did not significantly suppress the formation of low volatile condensable organic materials, although NO_x obviously suppressed the formation of products for nucleation. Secondly, NO_x did suppress the formation of low-volatility condensable organic materials via forming potentially more volatile compounds and in addition to that, the suppressed formation of condensable organic materials was compensated by the presence of SO_2, resulting in comparable SOA yield. Organic nitrates are a group of compounds formed at high NO_x, which have been proposed to be more volatile (Presto et al., 2005; Kroll et al., 2006). However, many organic nitrates formed by photooxidation in this study were highly oxidized organic molecules (HOMs) containing multi-functional groups besides nitrate group ($C_{7-10}H_{9-15}NO_{8-15}$). These compounds are expected to have low volatility and they are found to have an uptake coefficient on particles of ~1 (Pullinen et al., in preparation). Therefore, the suppressing effect of NO_x on SOA yield was mostly likely due to suppressed nucleation, i.e., the lack of particle surface as condensational sink. Due to the low particle surface area, the wall loss of condensable vapors in the experiment at high NO_x and low SO_2 was large (as shown by the large f_{corr} in Fig. S4) and therefore SOA mass yield was suppressed. If vapor wall loss is considered, the difference between the SOA yield at high NO_x and at low NO_x under low SO_2 conditions will be much reduced, as we found for high SO_2 cases (Fig. 3a). Under high SO_2 conditions, the influence of vapor wall loss on the difference in SOA yield between high NO_x and low NO_x was minor (1%-8%, Fig. S4) due to the larger particle surface area.

For limonene oxidation, similar results of NO_x suppressing the particle mass formation have been found in low SO_2 conditions (Fig. 3b). Yet, in high SO_2 conditions, the SOA yield from limonene oxidation at high NO_x was still significantly lower than that at low NO_x, which is different from the findings for α-pinene SOA. The cause of this difference is currently unknown. Our data of SOA yield suggest that the products formed from limonene oxidation at high NO_x seemed to have higher average volatility than that at low NO_x.

296   The suppression of SOA mass formation by NO_x under low SO_2 conditions agrees with previous studies

297   (Eddingsaas et al., 2012a; Wildt et al., 2014; Sarrafzadeh et al., 2016; Hatakeyama et al., 1991). For example, it

298   was found that high concentration of NO_x (tens of ppb) suppressed mass yield of SOA formed from

299   photooxidation of β-pinene, α-pinene and VOC emitted by Mediterranean trees (Wildt et al., 2014; Sarrafzadeh et

300   al., 2016). And on the basis of the results by Eddingsaas et al. (2012a), the SOA yield at high NO_x (referred to as

301   "high NO" by the authors) is lower than at low NO_x in the absence of seed aerosol.

302   Our finding that the difference in SOA yield between high NO_x and low NO_x conditions was highly

303   reduced at high SO_2 is also in line with the findings of some previous studies using seed aerosols (Sarrafzadeh et

304   al., 2016; Eddingsaas et al., 2012a). For example, Sarrafzadeh et al. (2016) found that in the presence of seed

305   aerosol, the suppressing effect of NO_x on the SOA yield from β-pinene photooxidation is substantially diminished

306   and SOA yield only decreases by 20-30% in the NO_x range of <1 ppb to 86 ppb at constant OH concentrations.

307   The data by Eddingsaas et al. (2012a) also showed that in presence of seed aerosol, the difference in the SOA

308   yield between low NO_x and high NO_x is much decreased. However, our finding is in contrast with the findings in

309   other studies (Presto et al., 2005; Ng et al., 2007; Han et al., 2016; Stirnweis et al., 2017), who reported much

310   lower SOA yield at high NO_x than at low NO_x in presence of seed. The different findings in these studies from

311   ours may be attributed to the difference in the reaction conditions such as VOC oxidation pathways (OH

312   oxidation vs. ozonolysis), VOC and NO_x concentration ranges, NO/NO_2, OH concentrations as well as organic

313   aerosol loading, which all affect SOA yield. The reaction conditions of this study often differ from those

314   described in the literature (see Table S2).

315   The difference in these conditions can result in both different apparent dependence on specific

316   parameters and the varied SOA yield. For example, SOA yield from α-pinene photooxidation at low NO_x in this

317   study appeared to be much lower than that in Eddingsaas et al. (2012a). The difference between the SOA yield in

318   this study and some of previous studies and between the values in the literature can be attributed to several

319   reasons: 1) RO_2 fates may be different. For example, in our study at low NO_x, RO_2+NO account for a large

320   fraction of RO_2 loss while in Eddingsaas et al. (2012a) RO_2+HO_2 is the dominant pathway of RO_2 loss. This

321   difference in RO_2 fates may affect oxidation products distribution. 2) The organic aerosol loading of this study is

322   much lower than that some of previous studies (e.g., Eddingsaas et al. (2012a)) (see Fig. S9). SOA yields in this

323   study were also plotted versus organic aerosol loading to better compare with previous studies (Fig. S8 and S9).

324   3) The total particle surface area in this study may also differ from previous studies, which may influence the

325   apparent SOA yield due to vapor wall loss (the total particle surface area is often not reported in many previous

326   studies to compare with). 4) RH of this study is different from many previous studies, which often used very low

327   RH (<10%). It is important to emphasize that reaction conditions including the NO_x as well as SO_2 concentration

328   range and RH in this study were chosen to be relevant to the anthropogenic-biogenic interactions in the ambient

329   atmosphere. In addition, difference in the organic aerosol density used in yield calculation should be taken into

330   account. In this study, SOA yield was derived using a density of 1 g cm^{-3} to better compare with many previous

331   studies (e.g., (Henry et al., 2012)), while in some other studies SOA yield was derived using different density

332   (e.g., 1.32 g cm^{-3} in Eddingsaas et al. (2012a)).

333   **3.3.2   Effect of SO_2**

334   For both α-pinene and limonene, SO_2 was found to enhance the SOA mass yield at given NO_x levels,
335   especially for the high NO_x cases (Fig. 3). The enhancing effect of SO_2 on particle mass formation can be
336   attributed to two reasons. Firstly, SO_2 oxidation induced new particle formation, which provided more surface
337   and volume for further condensation of organic vapors. This is consistent with the finding that the enhancement
338   of SOA yield by SO_2 was more significant at high NO_x when the enhancement in nucleation was also more
339   significant. Secondly, H_2SO_4 formed by photooxidation of SO_2 can enhance SOA formation via acid-catalyzed
340   heterogeneous uptake, an important SOA formation pathway initially found from isoprene photooxidation (Jang
341   et al., 2002; Lin et al., 2012; Surratt et al., 2007) and later also in the photooxidation of other compound such as
342   anthropogenic VOC (Chu et al., 2016; Liu et al., 2016). For the products from monoterpene oxidation, such an
343   acid-catalyzed effect may also occur (Northcross and Jang, 2007; Wang et al., 2012; Lal et al., 2012; Zhang et al.,
344   2006; Ding et al., 2011; Iinuma et al., 2009) and in this study, the particles were acidic with the molar ratio of
345   NH_4^+ to SO_4^{2-} around 1.5-1.8, although no aqueous phase was formed.

346   We found that the SOA yield in the limonene oxidation at a moderate SO_2 level (2 ppb) was comparable
347   to the yield at high SO_2 (15 ppb) when similar particle number concentrations in both cases were formed. Both
348   yields were significantly higher than the yield at low SO_2 (<0.05 ppb, see Fig. S10). This comparison suggests
349   that the effect in enhancing new particle formation by SO_2 seems to be more important compared to the particle
350   acidity effect. The role of SO_2 in new particle formation is similar to adding seed aerosol and providing particle
351   surface for organics to condense. Artificially added seed aerosol has been shown to enhance SOA formation from
352   α-pinene and β-pinene oxidation (Ehn et al., 2014; Sarrafzadeh et al., 2016; Eddingsaas et al., 2012a). In some
353   other studies, it was found that the SOA yield from α-pinene oxidation is independent of initial seed surface area
354   (McVay et al., 2016; Nah et al., 2016). The difference in the literature may be due to the range of total surface
355   area of particles, reaction conditions and chamber setup. For example, the peak particle-to-chamber surface ratio
356   for α-pinene photooxidation in this study was 7.7×10^{-5} at high NO_x and low SO_2, much lower than the aerosol
357   surface area range in the studies by Nah et al. (2016) and McVay et al. (2016). A lower particle-to-chamber
358   surface ratio can lead to a larger fraction of organics lost on chamber walls. Hence, providing additional particle
359   surface by adding seed particles can increase the condensation of organics on particles and thus increase SOA
360   yield. However, once the surface area is high enough to inhibit condensation of vapors on chamber walls, further
361   enhancement of particle surface will not significantly enhance the yield (Sarrafzadeh et al., 2016).

362   As mentioned above, the SOA yield at high NO_x and low SO_2 was significantly suppressed due to vapor
363   wall loss. If the influence of vapor wall loss is considered, the SOA yield at high NO_x and low SO_2 will be much
364   higher and thus the observed enhancement of SOA yield by SO_2 under high NO_x conditions will be much less
365   pronounced. Under low NO_x conditions, the influence of vapor wall loss on the difference in SOA yield between
366   high SO_2 and low SO_2 was minor (1%-7% for α-pinene and 5-32% for limonene, see Fig. S4) due to the larger
367   particle surface area.

368   Particle acidity may also play a role in affecting the SOA yield in the experiments with high SO_2. Particle
369   acidity was found to enhance the SOA yield from α-pinene photooxidation at high NO_x (Offenberg et al., 2009)
370   and "high NO" conditions (Eddingsaas et al., 2012a). Yet, in low NO_x condition, particle acidity was reported to
371   have no significant effect on the SOA yield from α-pinene photooxidation (Eddingsaas et al., 2012a; Han et al.,

2016). According to these findings, at low NO_x the enhancement of SOA yield in this study is attributed to the effect of facilitating nucleation and providing more particle surface by SO_2 photooxidation. At high NO_x, the effect in enhancing new particle formation by SO_2 photooxidation seems to be more important, although the effect of particle acidity resulted from SO_2 photooxidation may also play a role.

SO$_2$ has been proposed to also affect gas phase chemistry of organics by changing the HO_2/OH or forming SO_3 (Friedman et al., 2016). In this study, the effect of SO_2 on gas phase chemistry of organics was not significant because of the much lower reactivity of SO_2 with OH compared with α-pinene and limonene (Atkinson et al., 2004, 2006; Atkinson and Arey, 2003) and the low OH concentrations (2-3 orders of magnitude lower than those in the study by Friedman et al. (2016)). Moreover, reactions of RO_2 with SO_2 was also not important because the reaction rate constant is very low ($<10^{-14}$ molecule^{-1} cm^3 s^{-1}) (Lightfoot et al., 1992; Berndt et al., 2015). In addition, from the AMS data of SOA formed at high SO_2 no significant organic fragments containing sulfur were found. Also the fragment $CH_3SO_2^+$ from organic sulfate suggested by Farmer et al. (2010) was not detected in our data. The absence of organic sulfate tracers is likely due to the lack of aqueous phase in aerosol particles in this study. Therefore, the influence of SO_2 on gas phase chemistry of organics and further on SOA yield via affecting gas phase chemistry is not important in this study.

The presence of high SO_2 enhanced the SOA mass yield at high NO_x conditions, which was even comparable with the SOA yield at low NO_x for α-pinene oxidation. This finding indicates that the suppressing effect of NO_x on SOA mass formation was compensated to large extent by the presence of SO_2. This has important implications for SOA formation affected by anthropogenic-biogenic interactions in the real atmosphere when SO_2 and NO_x often co-exist in relative high concentrations as discussed below.

3.4   Effects of NO_x and SO_2 on SOA chemical composition

The effects of NO_x and SO_2 on SOA chemical composition were analyzed on the basis of AMS data. We found that NO_x enhanced nitrate formation. The ratio of the mass of nitrate to organics was higher at high NO_x than at low NO_x regardless of the SO_2 level, and similar trends were found for SOA from α-pinene and limonene oxidation (Fig. 4a). Higher nitrate to organics ratios were observed for SOA from limonene at high NO_x, which is mainly due to the lower VOC/NO_x ratio resulted from the lower concentrations of limonene (7 ppb) compared to α-pinene (20 ppb) (see Table 1). Overall, the mass ratios of nitrate to organics ranged from 0.02 to 0.11 considering all the experiments in this study.

Nitrate formed can be either inorganic (such as HNO_3 from the reaction of NO_2 with OH) or organic (from the reaction of RO_2 with NO). The ratio of NO_2^+ (*m/z*=46) to NO^+ (*m/z*=30) in the mass spectra detected by AMS can be used to differentiate whether nitrate is organic or inorganic (Fry et al., 2009; Rollins et al., 2009; Farmer et al., 2010; Kiendler-Scharr et al., 2016). Organic nitrate was considered to have a NO_2^+/NO^+ of ~0.1 and inorganic NH_4NO_3 had a NO_2^+/NO^+ of ~0.31 with the instrument used in this study as determined from calibration measurements. In this study, NO_2^+/NO^+ ratios ranged from 0.14 to 0.18, closer to the ratio of organic nitrate. The organic nitrate was estimated to account for 57%-77% (molar fraction) of total nitrate considering both the low NO_x and high NO_x conditions. This indicates that nitrate was mostly organic nitrate, even at low NO_x in this study.

409   In order to determine the contribution of organic nitrate to total organics, we estimated the molecular

410   weight of organic nitrates formed by α-pinene and limonene oxidation to be 200-300 g/mol, based on reaction

411   mechanisms ((Eddingsaas et al., 2012b) and MCM v3.3, via website: http://mcm.leeds.ac.uk/MCM.). We

412   assumed a molecular weight of 200 g/mol in order to make our results comparable to the field studies which used

413   similar molecular weight (Kiendler-Scharr et al., 2016). For this value, the organic nitrate compounds were

414   estimated to account for 7-26% of the total organics mass as measured by AMS in SOA. Organic nitrate fraction

415   in total organics was within the range of values found in a field observation in southeast US (5-12% in summer

416   and 9-25% in winter depending on the molecular weight of organic nitrate) using AMS (Xu et al., 2015b) and

417   particle organic nitrate content derived from the sum of speciated organic nitrates (around 1-17% considering

418   observed variability and 3% and 8% on average in the afternoon and at night, respectively) (Lee et al., 2016).

419   Note that the organic nitrate fraction observed in this study was lower than the mean value (42%) for a number of

420   European observation stations when organic nitrate is mainly formed by the reaction of VOC with NO_3

421   (Kiendler-Scharr et al., 2016).

422   Moreover, we found that the contribution of organic nitrate to total organics (calculated using a

423   molecular weight of 200 g/mol for organic nitrate) was higher at high NO_x (Fig. 4b), although in some

424   experiments the ratios of NO_2^+ to NO^+ were too noisy to derive a reliable fraction of organic nitrate. This result is

425   consistent with the reaction scheme that at high NO_x, almost all RO_2 loss was switched to the reaction with NO,

426   which is expected to enhance the organic nitrate formation. Besides organic nitrate, the ratio of nitrogen to carbon

427   atoms (N/C) was also found to be higher at high NO_x (Fig. S11). But after considering nitrate functional group

428   separately, N/C ratio was very low, generally <0.01, which indicates majority of the organic nitrogen existed in

429   the form of organic nitrate.

430   The chemical composition of organic components of SOA in terms of H/C and O/C ratios at different

431   NO_x and SO_2 levels was further compared. For SOA from α-pinene photooxidation, in low SO_2 conditions, no

432   significant difference in H/C and O/C was found between SOA formed at low NO_x and at high NO_x within the

433   experimental uncertainties (Fig. 5). The variability of H/C and O/C at high NO_x is large, mainly due to the low

434   particle mass and small particle size. In high SO_2 conditions, SOA formed at high NO_x had the higher O/C and

435   lower H/C, which indicates that SOA components had higher oxidation state. The higher O/C at high NO_x than at

436   low NO_x is partly due to the higher OH dose at high NO_x, although even at same OH dose O/C at high NO_x was

437   still slightly higher than at low NO_x in high SO_2 conditions.

438   For the SOA formed from limonene photooxidation, no significant difference in the H/C and O/C was

439   found between different NO_x and SO_2 conditions (Fig. S12), which is partly due to the low signal resulting from

440   low particle mass and small particle size in high NO_x conditions.

441   Due to the high uncertainties for some of the H/C and O/C data, the chemical composition was further

442   analyzed using f_{44} and f_{43} since f_{44} and f_{43} are less noisy (Fig. 6). For both α-pinene and limonene, SOA formed at

443   high NO_x generally had lower f_{43}. Because f_{43} generally correlates with H/C in organic aerosol (Ng et al., 2011),

444   lower f_{43} is indicative of lower H/C, which is consistent with the lower H/C at high NO_x observed for SOA from

445   α-pinene oxidation in high SO_2 conditions (Fig. 5). The lower f_{43} at high NO_x was evidenced in the oxidation of

446   α-pinene based on the data in a previous study (Chhabra et al., 2011). The lower H/C and f_{43} are likely to be

447   related to the reaction pathways. According to the reaction mechanism mentioned above, at low NO_x a significant

448 fraction of RO_2 reacted with HO_2 forming hydroperoxides, while at high NO_x almost all RO_2 reacted with NO

449 forming organic nitrates. Compared with organic nitrates, hydroperoxides have higher H/C ratio. The same

450 mechanism also caused higher organic nitrate fraction at high NO_x, as discussed above.

451   Detailed mass spectra of SOA were compared, shown in Fig 7. For α-pinene, in high SO_2 conditions,

452 mass spectra of SOA formed at high NO_x generally had higher intensity for CHOgt1 ("gt1" means greater than 1)

453 family ions, such as CO_2^+ (m/z 44), but lower intensity for CH family ions, such as $C_2H_3^+$ (m/z 15), $C_3H_3^+$ (m/z 39)

454 (Fig. 7b) than at low NO_x. In low SO_2 conditions, such difference is not apparent (Fig. 7a), partly due to the low

455 signal from AMS for SOA formed at high NO_x as discussed above. For both the high SO_2 and low SO_2 cases,

456 mass spectra of SOA at high NO_x show higher intensity of CHN1 family ions. This is also consistent with the

457 higher N/C ratio shown above. For SOA from limonene oxidation, SOA formed at high NO_x had lower mass

458 fraction at m/z 15 ($C_2H_3^+$), 28 (CO^+), 43 ($C_2H_3O^+$), 44 (CO_2^+), and higher mass fraction at m/z 27 (CHN^+, $C_2H_3^+$),

459 41 ($C_3H_5^+$), 55 ($C_4H_7^+$), 64 (C_4O^+) than at low NO_x (Fig. S13). It seems that overall mass spectra of the SOA from

460 limonene formed at high NO_x had higher intensity for CH family ions, but lower intensity for CHO1 family ions

461 than at low NO_x. Note that the differences in these m/z were based on the average spectra during the whole

462 reaction period and may not reflect the chemical composition at a certain time.

463 **4 Conclusion and implications**

464   We investigated the SOA formation from the photooxidation of α-pinene and limonene under different NO_x

465 and SO_2 conditions, when OH oxidation was the dominant oxidation pathway of monoterpenes. The fate of RO_2

466 was regulated by varying NO_x concentrations. We confirmed that NO_x suppressed new particle formation. NO_x

467 also suppressed SOA mass yield in the absence of SO_2. The suppression of SOA yield by NO_x was likely due to

468 the suppressed new particle formation, i.e., absence of sufficient particle surfaces for organic vapor to condense

469 on at high NO_x, which could result in large vapor loss to chamber walls.

470   SO_2 enhanced SOA yield from α-pinene and limonene photooxidation. SO_2 oxidation produced high number

471 concentration of particles and compensated for the suppression of SOA yield by NO_x to a large extent. The

472 enhancement of SOA yield by SO_2 is likely to be mainly caused by facilitating nucleation by H_2SO_4, although the

473 contribution of acid-catalyzed heterogeneous uptake cannot be excluded.

474   NO_x promoted nitrate formation. The majority (57-77%) of nitrate was organic nitrate at both low NO_x and

475 high NO_x, based on the estimate using the NO_2^+/NO^+ ratios from AMS data. The significant contribution of

476 organic nitrate to nitrate may have important implications for deriving the hygroscopicity from chemical

477 composition. For example, a number of studies derived the hygroscopicity parameter by linear combination of the

478 hygroscopicity parameters of various components such as sulfate, nitrate, and organics, assuming all nitrates are

479 inorganic nitrate (Wu et al., 2013; Cubison et al., 2008; Yeung et al., 2014; Bhattu and Tripathi, 2015; Jaatinen et

480 al., 2014; Moore et al., 2012; Gysel et al., 2007). Because the hygroscopicity parameter of organic nitrate may be

481 much lower than inorganic nitrate (Suda et al., 2014), such derivation may overestimate hygroscopicity.

482   Organic nitrate compounds are estimated to contribute 7-26% of the total organics using an average

483 molecular weight of 200 g/mol for organic nitrate compounds and a higher contribution of organic nitrate was

484 found at high NO_x. Generally, SOA formed at high NO_x has a lower H/C compared to that at low NO_x. The

485 higher contribution of organic nitrate to total organics and lower H/C at high NO_x than at low NO_x is attributed to

the reaction of RO_2 with NO, which produced more organic nitrates relative to organic hydroperoxides formed via the reaction of RO_2 with HO_2. The different chemical composition of SOA between high and low NO_x conditions may affect the physicochemical properties of SOA such as volatility, hygroscopicity, and optical properties and thus change the impact of SOA on environment and climate.

In this study, the influence of vapor wall loss on SOA yield was estimated although the SOA yields in this study were not corrected for vapor wall loss. We need to be cautious about the enhancement of the SOA yield by SO_2 under high NO_x conditions and the suppression of the SOA yield by NO_x under low SO_2 conditions. These effects will be less pronounced when vapor wall loss is considered because of the significant vapor loss to chamber walls rather than to particles at low particle surface concentration. Yet, the low particle surface concentration and thus low condensational sink of vapors to particle surface reflect some real cases in the atmosphere, because when the condensational sink by particle surface is low in the atmosphere, organic vapors will be lost to the next largest sink, e.g. dry deposition. Nevertheless, our important findings hold for the influence of NO_x and SO_2 on SOA new particle formation, mass yield, and chemical composition, showing indeed the interaction of anthropogenic and biogenic emissions in the process of SOA formation.

The different effects of NO_x and SO_2 on new particle formation and SOA mass yields have important implications for SOA formation affected by anthropogenic-biogenic interactions in the ambient atmosphere. When an air mass of anthropogenic origin is transported to an area enriched in biogenic VOC emissions or vice versa, anthropogenic-biogenic interactions occur. Such scenarios are common in the ambient atmosphere in many areas. For example, Kiendler-Scharr et al. (2016) shows that the organic nitrate concentrations are high in all the rural sites all over Europe, indicating the important influence of anthropogenic emissions in rural areas which are often enriched in biogenic emissions. [14]C analysis in several studies show that modern source carbon, from biogenic emission or biomass burning, account for large fractions of organic aerosol even in urban areas (Szidat et al., 2009; Weber et al., 2007; Sun et al., 2012), indicating the potential interactions of biogenic emissions with anthropogenic emissions in urban areas. In such cases, anthropogenic NO_x alone may suppress the new particle formation and SOA mass from biogenic VOC oxidation, as we found in this study, because in principle the suppression of SOA mass due to suppressed nucleation can occur in the ambient atmosphere, although chamber experiments often cannot accurately simulate the vapor loss on surface in the boundary layer. However, due to the co-existence of NO_x with SO_2, H_2SO_4 formed by SO_2 oxidation can counteract such suppression of particle mass because regardless of NO_x levels, H_2SO_4 can induce new particle formation especially in the presence of water, ammonia or amine (Berndt et al., 2005; Zhang et al., 2012; Sipila et al., 2010; Almeida et al., 2013; Kirkby et al., 2011; Chen et al., 2012). The overall effects on SOA mass depend on specific NO_x, SO_2 and VOC concentrations and VOC types as well as anthropogenic aerosol concentrations and can be a net suppressing, neutral, or enhancing effect. Such scheme is depicted in Fig. 8. Other anthropogenic emissions, such as primary anthropogenic aerosol and precursors of anthropogenic secondary aerosol, can have similar roles as SO_2. By affecting the concentrations of SO_2, NO_x, and anthropogenic aerosol, anthropogenic emissions may have important mediating impacts on biogenic SOA formation. Considering the effects of these factors in isolation may cause bias in predicting biogenic SOA concentrations. The combined impacts of SO_2, NO_x, and anthropogenic aerosol are also important to the estimate on how much organic aerosol concentrations will change with the ongoing and future reduction of anthropogenic emissions (Carlton et al., 2010).

Acknowledgements

References

Aiken, A. C., DeCarlo, P. F., and Jimenez, J. L.: Elemental analysis of organic species with electron ionization high-resolution mass spectrometry, Anal. Chem., 79, 8350-8358, 10.1021/ac071150w, 2007.

Aiken, A. C., Decarlo, P. F., Kroll, J. H., Worsnop, D. R., Huffman, J. A., Docherty, K. S., Ulbrich, I. M., Mohr, C., Kimmel, J. R., Sueper, D., Sun, Y., Zhang, Q., Trimborn, A., Northway, M., Ziemann, P. J., Canagaratna, M. R., Onasch, T. B., Alfarra, M. R., Prevot, A. S. H., Dommen, J., Duplissy, J., Metzger, A., Baltensperger, U., and Jimenez, J. L.: O/C and OM/OC ratios of primary, secondary, and ambient organic aerosols with high-resolution time-of-flight aerosol mass spectrometry, Environ. Sci. Technol., 42, 4478-4485, 10.1021/es703009q, 2008.

Almeida, J., Schobesberger, S., Kurten, A., Ortega, I. K., Kupiainen-Maatta, O., Praplan, A. P., Adamov, A., Amorim, A., Bianchi, F., Breitenlechner, M., David, A., Dommen, J., Donahue, N. M., Downard, A., Dunne, E., Duplissy, J., Ehrhart, S., Flagan, R. C., Franchin, A., Guida, R., Hakala, J., Hansel, A., Heinritzi, M., Henschel, H., Jokinen, T., Junninen, H., Kajos, M., Kangasluoma, J., Keskinen, H., Kupc, A., Kurten, T., Kvashin, A. N., Laaksonen, A., Lehtipalo, K., Leiminger, M., Leppa, J., Loukonen, V., Makhmutov, V., Mathot, S., McGrath, M. J., Nieminen, T., Olenius, T., Onnela, A., Petaja, T., Riccobono, F., Riipinen, I., Rissanen, M., Rondo, L., Ruuskanen, T., Santos, F. D., Sarnela, N., Schallhart, S., Schnitzhofer, R., Seinfeld, J. H., Simon, M., Sipila, M., Stozhkov, Y., Stratmann, F., Tome, A., Trostl, J., Tsagkogeorgas, G., Vaattovaara, P., Viisanen, Y., Virtanen, A., Vrtala, A., Wagner, P. E., Weingartner, E., Wex, H., Williamson, C., Wimmer, D., Ye, P. L., Yli-Juuti, T., Carslaw, K. S., Kulmala, M., Curtius, J., Baltensperger, U., Worsnop, D. R., Vehkamaki, H., and Kirkby, J.: Molecular understanding of sulphuric acid-amine particle nucleation in the atmosphere, Nature, 502, 359-+, 10.1038/nature12663, 2013.

Atkinson, R., and Arey, J.: Atmospheric degradation of volatile organic compounds, Chem. Rev., 103, 4605-4638, 10.1021/cr0206420, 2003.

Atkinson, R., Baulch, D. L., Cox, R. A., Crowley, J. N., Hampson, R. F., Hynes, R. G., Jenkin, M. E., Rossi, M. J., and Troe, J.: Evaluated kinetic and photochemical data for atmospheric chemistry: Volume I - gas phase reactions of O-x, HOx, NOx and SOx species, Atmos. Chem. Phys., 4, 1461-1738, 2004.

Atkinson, R., Baulch, D. L., Cox, R. A., Crowley, J. N., Hampson, R. F., Hynes, R. G., Jenkin, M. E., Rossi, M. J., and Troe, J.: Evaluated kinetic and photochemical data for atmospheric chemistry: Volume II - gas phase reactions of organic species, Atmos. Chem. Phys., 6, 3625-4055, 2006.

Berndt, T., Boge, O., Stratmann, F., Heintzenberg, J., and Kulmala, M.: Rapid formation of sulfuric acid particles at near-atmospheric conditions, Science, 307, 698-700, 10.1126/science.1104054, 2005.

Berndt, T., Richters, S., Kaethner, R., Voigtlander, J., Stratmann, F., Sipila, M., Kulmala, M., and Herrmann, H.: Gas-Phase Ozonolysis of Cycloalkenes: Formation of Highly Oxidized RO2 Radicals and Their Reactions with NO, NO2, SO2, and Other RO2 Radicals, J. Phys. Chem. A 119, 10336-10348, 10.1021/acs.jpca.5b07295, 2015.

Bhattu, D., and Tripathi, S. N.: CCN closure study: Effects of aerosol chemical composition and mixing state, J. Geophys. Res.-Atmos., 120, 766-783, 10.1002/2014jd021978, 2015.

Bohn, B., Rohrer, F., Brauers, T., and Wahner, A.: Actinometric measurements of NO2 photolysis frequencies in the atmosphere simulation chamber SAPHIR, Atmos. Chem. Phys., 5, 493-503, 2005.

Bohn, B., and Zilken, H.: Model-aided radiometric determination of photolysis frequencies in a sunlit atmosphere simulation chamber, Atmos. Chem. Phys., 5, 191-206, 2005.

568   Canagaratna, M. R., Jimenez, J. L., Kroll, J. H., Chen, Q., Kessler, S. H., Massoli, P., Hildebrandt Ruiz, L.,

569   Fortner, E., Williams, L. R., Wilson, K. R., Surratt, J. D., Donahue, N. M., Jayne, J. T., and Worsnop, D. R.:

570   Elemental ratio measurements of organic compounds using aerosol mass spectrometry: characterization,

571   improved calibration, and implications, Atmos. Chem. Phys., 15, 253-272, 10.5194/acp-15-253-2015, 2015.

572   Carlton, A. G., Wiedinmyer, C., and Kroll, J. H.: A review of Secondary Organic Aerosol (SOA) formation from

573   isoprene, Atmos. Chem. Phys., 9, 4987-5005, 2009.

574   Carlton, A. G., Pinder, R. W., Bhave, P. V., and Pouliot, G. A.: To What Extent Can Biogenic SOA be

575   Controlled?, Environ. Sci. Technol., 44, 3376-3380, 10.1021/es903506b, 2010.

576   Chen, M., Titcombe, M., Jiang, J. K., Jen, C., Kuang, C. A., Fischer, M. L., Eisele, F. L., Siepmann, J. I., Hanson,

577   D. R., Zhao, J., and McMurry, P. H.: Acid-base chemical reaction model for nucleation rates in the polluted

578   atmospheric boundary layer, Proc. Nat. Acad. Sci. U.S.A., 109, 18713-18718, 10.1073/pnas.1210285109, 2012.

579   Chhabra, P. S., Ng, N. L., Canagaratna, M. R., Corrigan, A. L., Russell, L. M., Worsnop, D. R., Flagan, R. C.,

580   and Seinfeld, J. H.: Elemental composition and oxidation of chamber organic aerosol, Atmos. Chem. Phys., 11,

581   8827-8845, 10.5194/acp-11-8827-2011, 2011.

582   Chu, B. W., Zhang, X., Liu, Y. C., He, H., Sun, Y., Jiang, J. K., Li, J. H., and Hao, J. M.: Synergetic formation of

583   secondary inorganic and organic aerosol: effect of SO2 and NH3 on particle formation and growth, Atmos.

584   Chem. Phys., 16, 14219-14230, 10.5194/acp-16-14219-2016, 2016.

585   Chung, S. H., and Seinfeld, J. H.: Global distribution and climate forcing of carbonaceous aerosols, J. Geophys.

586   Res.-Atmos., 107, 4407, 10.1029/2001jd001397, 2002.

587   Clegg, S. L., Brimblecombe, P., and Wexler, A. S.: Thermodynamic model of the system H+-NH4+-SO42--

588   NO3--H2O at tropospheric temperatures, J. Phys. Chem. A 102, 2137-2154, 10.1021/jp973042r, 1998.

589   Cubison, M. J., Ervens, B., Feingold, G., Docherty, K. S., Ulbrich, I. M., Shields, L., Prather, K., Hering, S., and

590   Jimenez, J. L.: The influence of chemical composition and mixing state of Los Angeles urban aerosol on CCN

591   number and cloud properties, Atmos. Chem. Phys., 8, 5649-5667, 10.5194/acp-8-5649-2008, 2008.

592   de Gouw, J. A., Middlebrook, A. M., Warneke, C., Goldan, P. D., Kuster, W. C., Roberts, J. M., Fehsenfeld, F.

593   C., Worsnop, D. R., Canagaratna, M. R., Pszenny, A. A. P., Keene, W. C., Marchewka, M., Bertman, S. B., and

594   Bates, T. S.: Budget of organic carbon in a polluted atmosphere: Results from the New England Air Quality

595   Study in 2002, J. Geophys. Res.-Atmos., 110, D16305, 10.1029/2004jd005623, 2005.

596   Ding, X. A., Wang, X. M., and Zheng, M.: The influence of temperature and aerosol acidity on biogenic

597   secondary organic aerosol tracers: Observations at a rural site in the central Pearl River Delta region, South

598   China, Atmos. Environ., 45, 1303-1311, 10.1016/j.atmosenv.2010.11.057, 2011.

599   Draper, D. C., Farmer, D. K., Desyaterik, Y., and Fry, J. L.: A qualitative comparison of secondary organic

600   aerosol yields and composition from ozonolysis of monoterpenes at varying concentrations of NO2, Atmos.

601   Chem. Phys., 15, 12267-12281, 10.5194/acp-15-12267-2015, 2015.

602   Eddingsaas, N. C., Loza, C. L., Yee, L. D., Chan, M., Schilling, K. A., Chhabra, P. S., Seinfeld, J. H., and

603   Wennberg, P. O.: alpha-pinene photooxidation under controlled chemical conditions - Part 2: SOA yield and

604   composition in low- and high-NOx environments, Atmos. Chem. Phys., 12, 7413-7427, 10.5194/acp-12-7413-

605   2012, 2012a.

606   Eddingsaas, N. C., Loza, C. L., Yee, L. D., Seinfeld, J. H., and Wennberg, P. O.: alpha-pinene photooxidation
607   under controlled chemical conditions - Part 1: Gas-phase composition in low- and high-NOx environments,
608   Atmos. Chem. Phys., 12, 6489-6504, 10.5194/acp-12-6489-2012, 2012b.

609   Ehn, M., Thornton, J. A., Kleist, E., Sipila, M., Junninen, H., Pullinen, I., Springer, M., Rubach, F., Tillmann, R.,
610   Lee, B., Lopez-Hilfiker, F., Andres, S., Acir, I. H., Rissanen, M., Jokinen, T., Schobesberger, S., Kangasluoma,
611   J., Kontkanen, J., Nieminen, T., Kurten, T., Nielsen, L. B., Jorgensen, S., Kjaergaard, H. G., Canagaratna, M.,
612   Dal Maso, M., Berndt, T., Petaja, T., Wahner, A., Kerminen, V. M., Kulmala, M., Worsnop, D. R., Wildt, J., and
613   Mentel, T. F.: A large source of low-volatility secondary organic aerosol, Nature, 506, 476-479,
614   10.1038/nature13032, 2014.

615   Emanuelsson, E. U., Hallquist, M., Kristensen, K., Glasius, M., Bohn, B., Fuchs, H., Kammer, B., Kiendler-
616   Scharr, A., Nehr, S., Rubach, F., Tillmann, R., Wahner, A., Wu, H. C., and Mentel, T. F.: Formation of
617   anthropogenic secondary organic aerosol (SOA) and its influence on biogenic SOA properties, Atmos. Chem.
618   Phys., 13, 2837-2855, 10.5194/acp-13-2837-2013, 2013.

619   Farmer, D. K., Matsunaga, A., Docherty, K. S., Surratt, J. D., Seinfeld, J. H., Ziemann, P. J., and Jimenez, J. L.:
620   Response of an aerosol mass spectrometer to organonitrates and organosulfates and implications for atmospheric
621   chemistry, Proc. Nat. Acad. Sci. U.S.A., 107, 6670-6675, 10.1073/pnas.0912340107, 2010.

622   Finlayson-Pitts, B. J., and Pitts Jr., J. N.: Chemistry of the upper and lower atmosphere: theory, experiments, and
623   applications, Academic Press, San Diego, 969 pp., 1999.

624   Flores, J. M., Zhao, D. F., Segev, L., Schlag, P., Kiendler-Scharr, A., Fuchs, H., Watne, A. K., Bluvshtein, N.,
625   Mentel, T. F., Hallquist, M., and Rudich, Y.: Evolution of the complex refractive index in the UV spectral region
626   in ageing secondary organic aerosol, Atmos. Chem. Phys., 14, 5793-5806, 10.5194/acp-14-5793-2014, 2014.

627   Friedman, B., Brophy, P., Brune, W. H., and Farmer, D. K.: Anthropogenic Sulfur Perturbations on Biogenic
628   Oxidation: SO2 Additions Impact Gas-Phase OH Oxidation Products of alpha- and beta-Pinene, Environ. Sci.
629   Technol., 50, 1269-1279, 10.1021/acs.est.5b05010, 2016.

630   Fry, J. L., Kiendler-Scharr, A., Rollins, A. W., Wooldridge, P. J., Brown, S. S., Fuchs, H., Dube, W., Mensah, A.,
631   dal Maso, M., Tillmann, R., Dorn, H. P., Brauers, T., and Cohen, R. C.: Organic nitrate and secondary organic
632   aerosol yield from NO3 oxidation of beta-pinene evaluated using a gas-phase kinetics/aerosol partitioning model,
633   Atmos. Chem. Phys., 9, 1431-1449, 2009.

634   Fuchs, H., Dorn, H. P., Bachner, M., Bohn, B., Brauers, T., Gomm, S., Hofzumahaus, A., Holland, F., Nehr, S.,
635   Rohrer, F., Tillmann, R., and Wahner, A.: Comparison of OH concentration measurements by DOAS and LIF
636   during SAPHIR chamber experiments at high OH reactivity and low NO concentration, Atmos. Meas. Tech., 5,
637   1611-1626, 10.5194/amt-5-1611-2012, 2012.

638   Glasius, M., la Cour, A., and Lohse, C.: Fossil and nonfossil carbon in fine particulate matter: A study of five
639   European cities, Journal of Geophysical Research: Atmospheres, 116, D11302, 10.1029/2011jd015646, 2011.

640   Goldstein, A. H., Koven, C. D., Heald, C. L., and Fung, I. Y.: Biogenic carbon and anthropogenic pollutants
641   combine to form a cooling haze over the southeastern United States, Proc. Nat. Acad. Sci. U.S.A., 106, 8835-
642   8840, 10.1073/pnas.0904128106, 2009.

643   Griffin, R. J., Cocker, D. R., Flagan, R. C., and Seinfeld, J. H.: Organic aerosol formation from the oxidation of
644   biogenic hydrocarbons, J. Geophys. Res.-Atmos., 104, 3555-3567, 10.1029/1998jd100049, 1999.

645 Guenther, A., Hewitt, C. N., Erickson, D., Fall, R., Geron, C., Graedel, T., Harley, P., Klinger, L., Lerdau, M.,
646 McKay, W. A., Pierce, T., Scholes, B., Steinbrecher, R., Tallamraju, R., Taylor, J., and Zimmerman, P.: A
647 global-model of natural volatile organic-compound emissions, J. Geophys. Res.-Atmos., 100, 8873-8892,
648 10.1029/94jd02950, 1995.

649 Guenther, A. B., Jiang, X., Heald, C. L., Sakulyanontvittaya, T., Duhl, T., Emmons, L. K., and Wang, X.: The
650 Model of Emissions of Gases and Aerosols from Nature version 2.1 (MEGAN2.1): an extended and updated
651 framework for modeling biogenic emissions, Geosci. Model Dev., 5, 1471-1492, 10.5194/gmd-5-1471-2012,
652 2012.

653 Gysel, M., Crosier, J., Topping, D. O., Whitehead, J. D., Bower, K. N., Cubison, M. J., Williams, P. I., Flynn, M.
654 J., McFiggans, G. B., and Coe, H.: Closure study between chemical composition and hygroscopic growth of
655 aerosol particles during TORCH2, Atmos. Chem. Phys., 7, 6131-6144, 2007.

656 Hallquist, M., Wenger, J. C., Baltensperger, U., Rudich, Y., Simpson, D., Claeys, M., Dommen, J., Donahue, N.
657 M., George, C., Goldstein, A. H., Hamilton, J. F., Herrmann, H., Hoffmann, T., Iinuma, Y., Jang, M., Jenkin, M.
658 E., Jimenez, J. L., Kiendler-Scharr, A., Maenhaut, W., McFiggans, G., Mentel, T. F., Monod, A., Prevot, A. S.
659 H., Seinfeld, J. H., Surratt, J. D., Szmigielski, R., and Wildt, J.: The formation, properties and impact of
660 secondary organic aerosol: current and emerging issues, Atmos. Chem. Phys., 9, 5155-5236, 2009.

661 Han, Y. M., Stroud, C. A., Liggio, J., and Li, S. M.: The effect of particle acidity on secondary organic aerosol
662 formation from alpha-pinene photooxidation under atmospherically relevant conditions, Atmos. Chem. Phys., 16,
663 13929-13944, 10.5194/acp-16-13929-2016, 2016.

664 Hatakeyama, S., Izumi, K., Fukuyama, T., Akimoto, H., and Washida, N.: Reactions of oh with alpha-pinene and
665 beta-pinene in air - estimate of global co production from the atmospheric oxidation of terpenes, J. Geophys.
666 Res.-Atmos., 96, 947-958, 10.1029/90jd02341, 1991.

667 Henry, K. M., Lohaus, T., and Donahue, N. M.: Organic Aerosol Yields from alpha-Pinene Oxidation: Bridging
668 the Gap between First-Generation Yields and Aging Chemistry, Environ. Sci. Technol., 46, 12347-12354,
669 10.1021/es302060y, 2012.

670 Hoffmann, T., Odum, J. R., Bowman, F., Collins, D., Klockow, D., Flagan, R. C., and Seinfeld, J. H.: Formation
671 of organic aerosols from the oxidation of biogenic hydrocarbons, J. Atmos. Chem., 26, 189-222,
672 10.1023/a:1005734301837, 1997.

673 Hoyle, C. R., Boy, M., Donahue, N. M., Fry, J. L., Glasius, M., Guenther, A., Hallar, A. G., Hartz, K. H., Petters,
674 M. D., Petaja, T., Rosenoern, T., and Sullivan, A. P.: A review of the anthropogenic influence on biogenic
675 secondary organic aerosol, Atmos. Chem. Phys., 11, 321-343, DOI 10.5194/acp-11-321-2011, 2011.

676 Iinuma, Y., Boege, O., Kahnt, A., and Herrmann, H.: Laboratory chamber studies on the formation of
677 organosulfates from reactive uptake of monoterpene oxides, Phys. Chem. Chem. Phys., 11, 7985-7997,
678 10.1039/b904025k, 2009.

679 Jaatinen, A., Romakkaniemi, S., Anttila, T., Hyvarinen, A. P., Hao, L. Q., Kortelainen, A., Miettinen, P.,
680 Mikkonen, S., Smith, J. N., Virtanen, A., and Laaksonen, A.: The third Pallas Cloud Experiment: Consistency
681 between the aerosol hygroscopic growth and CCN activity, Boreal Environment Research, 19, 368-382, 2014.

682 Jang, M. S., Czoschke, N. M., Lee, S., and Kamens, R. M.: Heterogeneous atmospheric aerosol production by
683 acid-catalyzed particle-phase reactions, Science, 298, 814-817, 10.1126/science.1075798, 2002.

684 Jenkin, M. E., Saunders, S. M., and Pilling, M. J.: The tropospheric degradation of volatile organic compounds: A

685 protocol for mechanism development, Atmos. Environ., 31, 81-104, 10.1016/s1352-2310(96)00105-7, 1997.

686 Jimenez, J. L., Canagaratna, M. R., Donahue, N. M., Prevot, A. S. H., Zhang, Q., Kroll, J. H., DeCarlo, P. F.,

687 Allan, J. D., Coe, H., Ng, N. L., Aiken, A. C., Docherty, K. S., Ulbrich, I. M., Grieshop, A. P., Robinson, A. L.,

688 Duplissy, J., Smith, J. D., Wilson, K. R., Lanz, V. A., Hueglin, C., Sun, Y. L., Tian, J., Laaksonen, A.,

689 Raatikainen, T., Rautiainen, J., Vaattovaara, P., Ehn, M., Kulmala, M., Tomlinson, J. M., Collins, D. R., Cubison,

690 M. J., Dunlea, E. J., Huffman, J. A., Onasch, T. B., Alfarra, M. R., Williams, P. I., Bower, K., Kondo, Y.,

691 Schneider, J., Drewnick, F., Borrmann, S., Weimer, S., Demerjian, K., Salcedo, D., Cottrell, L., Griffin, R.,

692 Takami, A., Miyoshi, T., Hatakeyama, S., Shimono, A., Sun, J. Y., Zhang, Y. M., Dzepina, K., Kimmel, J. R.,

693 Sueper, D., Jayne, J. T., Herndon, S. C., Trimborn, A. M., Williams, L. R., Wood, E. C., Middlebrook, A. M.,

694 Kolb, C. E., Baltensperger, U., and Worsnop, D. R.: Evolution of Organic Aerosols in the Atmosphere, Science,

695 326, 1525-1529, 10.1126/science.1180353, 2009.

696 Kanakidou, M., Seinfeld, J. H., Pandis, S. N., Barnes, I., Dentener, F. J., Facchini, M. C., Van Dingenen, R.,

697 Ervens, B., Nenes, A., Nielsen, C. J., Swietlicki, E., Putaud, J. P., Balkanski, Y., Fuzzi, S., Horth, J., Moortgat, G.

698 K., Winterhalter, R., Myhre, C. E. L., Tsigaridis, K., Vignati, E., Stephanou, E. G., and Wilson, J.: Organic

699 aerosol and global climate modelling: a review, Atmos. Chem. Phys., 5, 1053-1123, 2005.

700 Kiendler-Scharr, A., Mensah, A. A., Friese, E., Topping, D., Nemitz, E., Prevot, A. S. H., Äijälä, M., Allan, J.,

701 Canonaco, F., Canagaratna, M., Carbone, S., Crippa, M., Dall Osto, M., Day, D. A., De Carlo, P., Di Marco, C.

702 F., Elbern, H., Eriksson, A., Freney, E., Hao, L., Herrmann, H., Hildebrandt, L., Hillamo, R., Jimenez, J. L.,

703 Laaksonen, A., McFiggans, G., Mohr, C., O'Dowd, C., Otjes, R., Ovadnevaite, J., Pandis, S. N., Poulain, L.,

704 Schlag, P., Sellegri, K., Swietlicki, E., Tiitta, P., Vermeulen, A., Wahner, A., Worsnop, D., and Wu, H. C.:

705 Ubiquity of organic nitrates from nighttime chemistry in the European submicron aerosol, Geophys. Res. Lett.,

706 43, 7735-7744, 10.1002/2016GL069239, 2016.

707 Kirkby, J., Curtius, J., Almeida, J., Dunne, E., Duplissy, J., Ehrhart, S., Franchin, A., Gagne, S., Ickes, L., Kurten,

708 A., Kupc, A., Metzger, A., Riccobono, F., Rondo, L., Schobesberger, S., Tsagkogeorgas, G., Wimmer, D.,

709 Amorim, A., Bianchi, F., Breitenlechner, M., David, A., Dommen, J., Downard, A., Ehn, M., Flagan, R. C.,

710 Haider, S., Hansel, A., Hauser, D., Jud, W., Junninen, H., Kreissl, F., Kvashin, A., Laaksonen, A., Lehtipalo, K.,

711 Lima, J., Lovejoy, E. R., Makhmutov, V., Mathot, S., Mikkila, J., Minginette, P., Mogo, S., Nieminen, T.,

712 Onnela, A., Pereira, P., Petaja, T., Schnitzhofer, R., Seinfeld, J. H., Sipila, M., Stozhkov, Y., Stratmann, F.,

713 Tome, A., Vanhanen, J., Viisanen, Y., Vrtala, A., Wagner, P. E., Walther, H., Weingartner, E., Wex, H., Winkler,

714 P. M., Carslaw, K. S., Worsnop, D. R., Baltensperger, U., and Kulmala, M.: Role of sulphuric acid, ammonia and

715 galactic cosmic rays in atmospheric aerosol nucleation, Nature, 476, 429-U477, 10.1038/nature10343, 2011.

716 Kirkby, J., Duplissy, J., Sengupta, K., Frege, C., Gordon, H., Williamson, C., Heinritzi, M., Simon, M., Yan, C.,

717 Almeida, J., Tröstl, J., Nieminen, T., Ortega, I. K., Wagner, R., Adamov, A., Amorim, A., Bernhammer, A.-K.,

718 Bianchi, F., Breitenlechner, M., Brilke, S., Chen, X., Craven, J., Dias, A., Ehrhart, S., Flagan, R. C., Franchin, A.,

719 Fuchs, C., Guida, R., Hakala, J., Hoyle, C. R., Jokinen, T., Junninen, H., Kangasluoma, J., Kim, J., Krapf, M.,

720 Kürten, A., Laaksonen, A., Lehtipalo, K., Makhmutov, V., Mathot, S., Molteni, U., Onnela, A., Peräkylä, O.,

721 Piel, F., Petäjä, T., Praplan, A. P., Pringle, K., Rap, A., Richards, N. A. D., Riipinen, I., Rissanen, M. P., Rondo,

722 L., Sarnela, N., Schobesberger, S., Scott, C. E., Seinfeld, J. H., Sipilä, M., Steiner, G., Stozhkov, Y., Stratmann,

20

723 F., Tomé, A., Virtanen, A., Vogel, A. L., Wagner, A. C., Wagner, P. E., Weingartner, E., Wimmer, D., Winkler,

724 P. M., Ye, P., Zhang, X., Hansel, A., Dommen, J., Donahue, N. M., Worsnop, D. R., Baltensperger, U., Kulmala,

725 M., Carslaw, K. S., and Curtius, J.: Ion-induced nucleation of pure biogenic particles, Nature, 533, 521-526,

726 10.1038/nature17953, 2016.

727 Kleindienst, T. E., Edney, E. O., Lewandowski, M., Offenberg, J. H., and Jaoui, M.: Secondary organic carbon

728 and aerosol yields from the irradiations of isoprene and alpha-pinene in the presence of NOx and SO2, Environ.

729 Sci. Technol., 40, 3807-3812, 10.1021/es052446r, 2006.

730 Krechmer, J. E., Pagonis, D., Ziemann, P. J., and Jimenez, J. L.: Quantification of Gas-Wall Partitioning in

731 Teflon Environmental Chambers Using Rapid Bursts of Low-Volatility Oxidized Species Generated in Situ,

732 Environ. Sci. Technol., 50, 5757-5765, 10.1021/acs.est.6b00606, 2016.

733 Kroll, J. H., Ng, N. L., Murphy, S. M., Flagan, R. C., and Seinfeld, J. H.: Secondary organic aerosol formation

734 from isoprene photooxidation, Environ. Sci. Technol., 40, 1869-1877, 10.1021/es0524301, 2006.

735 Kroll, J. H., Chan, A. W. H., Ng, N. L., Flagan, R. C., and Seinfeld, J. H.: Reactions of semivolatile organics and

736 their effects on secondary organic aerosol formation, Environ. Sci. Technol., 41, 3545-3550, 10.1021/es062059x,

737 2007.

738 Lal, V., Khalizov, A. F., Lin, Y., Galvan, M. D., Connell, B. T., and Zhang, R. Y.: Heterogeneous Reactions of

739 Epoxides in Acidic Media, J. Phys. Chem. A 116, 6078-6090, 10.1021/jp2112704, 2012.

740 Lee, B. H., Mohr, C., Lopez-Hilfiker, F. D., Lutz, A., Hallquist, M., Lee, L., Romer, P., Cohen, R. C., Iyer, S.,

741 Kurten, T., Hu, W., Day, D. A., Campuzano-Jost, P., Jimenez, J. L., Xu, L., Ng, N. L., Guo, H., Weber, R. J.,

742 Wild, R. J., Brown, S. S., Koss, A., de Gouw, J., Olson, K., Goldstein, A. H., Seco, R., Kim, S., McAvey, K.,

743 Shepson, P. B., Starn, T., Baumann, K., Edgerton, E. S., Liu, J., Shilling, J. E., Miller, D. O., Brune, W.,

744 Schobesberger, S., D'Ambro, E. L., and Thornton, J. A.: Highly functionalized organic nitrates in the southeast

745 United States: Contribution to secondary organic aerosol and reactive nitrogen budgets, Proc. Nat. Acad. Sci.

746 U.S.A., 113, 1516-1521, 10.1073/pnas.1508108113, 2016.

747 Lightfoot, P. D., Cox, R. A., Crowley, J. N., Destriau, M., Hayman, G. D., Jenkin, M. E., Moortgat, G. K., and

748 Zabel, F.: Organic peroxy-radicals - kinetics, spectroscopy and tropospheric chemistry, Atmospheric

749 Environment Part a-General Topics, 26, 1805-1961, 10.1016/0960-1686(92)90423-i, 1992.

750 Lin, Y. H., Zhang, Z. F., Docherty, K. S., Zhang, H. F., Budisulistiorini, S. H., Rubitschun, C. L., Shaw, S. L.,

751 Knipping, E. M., Edgerton, E. S., Kleindienst, T. E., Gold, A., and Surratt, J. D.: Isoprene Epoxydiols as

752 Precursors to Secondary Organic Aerosol Formation: Acid-Catalyzed Reactive Uptake Studies with Authentic

753 Compounds, Environ. Sci. Technol., 46, 250-258, 10.1021/es202554c, 2012.

754 Liu, T., Wang, X., Hu, Q., Deng, W., Zhang, Y., Ding, X., Fu, X., Bernard, F., Zhang, Z., Lu, S., He, Q., Bi, X.,

755 Chen, J., Sun, Y., Yu, J., Peng, P., Sheng, G., and Fu, J.: Formation of secondary aerosols from gasoline vehicle

756 exhaust when mixing with SO2, Atmos. Chem. Phys., 16, 675-689, 10.5194/acp-16-675-2016, 2016.

757 Loza, C. L., Chan, A. W. H., Galloway, M. M., Keutsch, F. N., Flagan, R. C., and Seinfeld, J. H.:

758 Characterization of Vapor Wall Loss in Laboratory Chambers, Environ. Sci. Technol., 44, 5074-5078,

759 10.1021/es100727v, 2010.

Matsunaga, A., and Ziemann, P. J.: Gas-Wall Partitioning of Organic Compounds in a Teflon Film Chamber and Potential Effects on Reaction Product and Aerosol Yield Measurements, Aerosol Sci. Technol., 44, 881-892, 10.1080/02786826.2010.501044, 2010.

McVay, R. C., Zhang, X., Aumont, B., Valorso, R., Camredon, M., La, Y. S., Wennberg, P. O., and Seinfeld, J. H.: SOA formation from the photooxidation of alpha-pinene: systematic exploration of the simulation of chamber data, Atmos. Chem. Phys., 16, 2785-2802, 10.5194/acp-16-2785-2016, 2016.

Moore, R. H., Cerully, K., Bahreini, R., Brock, C. A., Middlebrook, A. M., and Nenes, A.: Hygroscopicity and composition of California CCN during summer 2010, J. Geophys. Res.-Atmos., 117, D00v12, 10.1029/2011jd017352, 2012.

Nah, T., McVay, R. C., Zhang, X., Boyd, C. M., Seinfeld, J. H., and Ng, N. L.: Influence of seed aerosol surface area and oxidation rate on vapor wall deposition and SOA mass yields: a case study with alpha-pinene ozonolysis, Atmos. Chem. Phys., 16, 9361-9379, 10.5194/acp-16-9361-2016, 2016.

Ng, N. L., Chhabra, P. S., Chan, A. W. H., Surratt, J. D., Kroll, J. H., Kwan, A. J., McCabe, D. C., Wennberg, P. O., Sorooshian, A., Murphy, S. M., Dalleska, N. F., Flagan, R. C., and Seinfeld, J. H.: Effect of NO(x) level on secondary organic aerosol (SOA) formation from the photooxidation of terpenes, Atmos. Chem. Phys., 7, 5159-5174, 2007.

Ng, N. L., Canagaratna, M. R., Jimenez, J. L., Chhabra, P. S., Seinfeld, J. H., and Worsnop, D. R.: Changes in organic aerosol composition with aging inferred from aerosol mass spectra, Atmos. Chem. Phys., 11, 6465-6474, 10.5194/acp-11-6465-2011, 2011.

Northcross, A. L., and Jang, M.: Heterogeneous SOA yield from ozonolysis of monoterpenes in the presence of inorganic acid, Atmos. Environ., 41, 1483-1493, 10.1016/j.atmosenv.2006.10.009, 2007.

Offenberg, J. H., Lewandowski, M., Edney, E. O., Kleindienst, T. E., and Jaoui, M.: Influence of Aerosol Acidity on the Formation of Secondary Organic Aerosol from Biogenic Precursor Hydrocarbons, Environ. Sci. Technol., 43, 7742-7747, 10.1021/es901538e, 2009.

Pandis, S. N., Paulson, S. E., Seinfeld, J. H., and Flagan, R. C.: Aerosol formation in the photooxidation of isoprene and beta-pinene, Atmospheric Environment Part a-General Topics, 25, 997-1008, 10.1016/0960-1686(91)90141-s, 1991.

Presto, A. A., Hartz, K. E. H., and Donahue, N. M.: Secondary organic aerosol production from terpene ozonolysis. 2. Effect of NOx concentration, Environ. Sci. Technol., 39, 7046-7054, 10.1021/es050400s, 2005.

Rohrer, F., Bohn, B., Brauers, T., Bruning, D., Johnen, F. J., Wahner, A., and Kleffmann, J.: Characterisation of the photolytic HONO-source in the atmosphere simulation chamber SAPHIR, Atmos. Chem. Phys., 5, 2189-2201, 2005.

Rollins, A. W., Kiendler-Scharr, A., Fry, J. L., Brauers, T., Brown, S. S., Dorn, H. P., Dube, W. P., Fuchs, H., Mensah, A., Mentel, T. F., Rohrer, F., Tillmann, R., Wegener, R., Wooldridge, P. J., and Cohen, R. C.: Isoprene oxidation by nitrate radical: alkyl nitrate and secondary organic aerosol yields, Atmos. Chem. Phys., 9, 6685-6703, 2009.

Sarrafzadeh, M., Wildt, J., Pullinen, I., Springer, M., Kleist, E., Tillmann, R., Schmitt, S. H., Wu, C., Mentel, T. F., Zhao, D. F., Hastie, D. R., and Kiendler-Scharr, A.: Impact of NOx and OH on secondary organic aerosol

798 formation from beta-pinene photooxidation, Atmos. Chem. Phys., 16, 11237-11248, 10.5194/acp-16-11237-2016,

799 2016.

800 Saunders, S. M., Jenkin, M. E., Derwent, R. G., and Pilling, M. J.: Protocol for the development of the Master

801 Chemical Mechanism, MCM v3 (Part A): tropospheric degradation of non-aromatic volatile organic compounds,

802 Atmos. Chem. Phys., 3, 161-180, 2003.

803 Shilling, J. E., Zaveri, R. A., Fast, J. D., Kleinman, L., Alexander, M. L., Canagaratna, M. R., Fortner, E., Hubbe,

804 J. M., Jayne, J. T., Sedlacek, A., Setyan, A., Springston, S., Worsnop, D. R., and Zhang, Q.: Enhanced SOA

805 formation from mixed anthropogenic and biogenic emissions during the CARES campaign, Atmos. Chem. Phys.

806 Discuss., 12, 26297-26349, 10.5194/acpd-12-26297-2012, 2012.

807 Sipila, M., Berndt, T., Petaja, T., Brus, D., Vanhanen, J., Stratmann, F., Patokoski, J., Mauldin, R. L., Hyvarinen,

808 A. P., Lihavainen, H., and Kulmala, M.: The Role of Sulfuric Acid in Atmospheric Nucleation, Science, 327,

809 1243-1246, 10.1126/science.1180315, 2010.

810 Spracklen, D. V., Jimenez, J. L., Carslaw, K. S., Worsnop, D. R., Evans, M. J., Mann, G. W., Zhang, Q.,

811 Canagaratna, M. R., Allan, J., Coe, H., McFiggans, G., Rap, A., and Forster, P.: Aerosol mass spectrometer

812 constraint on the global secondary organic aerosol budget, Atmos. Chem. Phys., 11, 12109-12136, 10.5194/acp-

813 11-12109-2011, 2011.

814 Stirnweis, L., Marcolli, C., Dommen, J., Barmet, P., Frege, C., Platt, S. M., Bruns, E. A., Krapf, M., Slowik, J.

815 G., Wolf, R., Prevot, A. S. H., Baltensperger, U., and El-Haddad, I.: Assessing the influence of NOx

816 concentrations and relative humidity on secondary organic aerosol yields from alpha-pinene photo-oxidation

817 through smog chamber experiments and modelling calculations, Atmos. Chem. Phys., 17, 5035-5061,

818 10.5194/acp-17-5035-2017, 2017.

819 Suda, S. R., Petters, M. D., Yeh, G. K., Strollo, C., Matsunaga, A., Faulhaber, A., Ziemann, P. J., Prenni, A. J.,

820 Carrico, C. M., Sullivan, R. C., and Kreidenweis, S. M.: Influence of Functional Groups on Organic Aerosol

821 Cloud Condensation Nucleus Activity, Environ. Sci. Technol., 48, 10182-10190, 10.1021/es502147y, 2014.

822 Sun, X. S., Hu, M., Guo, S., Liu, K. X., and Zhou, L. P.: C-14-Based source assessment of carbonaceous aerosols

823 at a rural site, Atmos. Environ., 50, 36-40, 10.1016/j.atmosenv.2012.01.008, 2012.

824 Surratt, J. D., Lewandowski, M., Offenberg, J. H., Jaoui, M., Kleindienst, T. E., Edney, E. O., and Seinfeld, J. H.:

825 Effect of acidity on secondary organic aerosol formation from isoprene, Environ. Sci. Technol., 41, 5363-5369,

826 10.1021/es0704176, 2007.

827 Szidat, S., Ruff, M., Perron, N., Wacker, L., Synal, H. A., Hallquist, M., Shannigrahi, A. S., Yttri, K. E., Dye, C.,

828 and Simpson, D.: Fossil and non-fossil sources of organic carbon (OC) and elemental carbon (EC) in Goteborg,

829 Sweden, Atmos. Chem. Phys., 9, 1521-1535, 10.5194/acp-9-1805-2009, 2009.

830 Wang, T. H., Liu, Z., Wang, W. G., and Ge, M. F.: Heterogeneous Uptake Kinetics of Limonene and Limonene

831 Oxide by Sulfuric Acid Solutions, Acta Phys. Chim. Sin. , 28, 1608-1614, 10.3866/pku.whxb201204241, 2012.

832 Weber, R. J., Sullivan, A. P., Peltier, R. E., Russell, A., Yan, B., Zheng, M., de Gouw, J., Warneke, C., Brock, C.,

833 Holloway, J. S., Atlas, E. L., and Edgerton, E.: A study of secondary organic aerosol formation in the

834 anthropogenic-influenced southeastern United States, J. Geophys. Res.-Atmos., 112, D13302,

835 10.1029/2007jd008408, 2007.

836 Wennberg, P. O.: Let's abandon the "high NOx" and "low NOx" terminology, IGAC News, 3−4, 2013.

837   Wexler, A. S., and Clegg, S. L.: Atmospheric aerosol models for systems including the ions H+, NH4+, Na+,
838   SO42-, NO3-,Cl-, Br-, and H2O, J. Geophys. Res.-Atmos., 107, 4207, 10.1029/2001jd000451, 2002.

839   Wildt, J., Mentel, T. F., Kiendler-Scharr, A., Hoffmann, T., Andres, S., Ehn, M., Kleist, E., Müsgen, P., Rohrer,
840   F., Rudich, Y., Springer, M., Tillmann, R., and Wahner, A.: Suppression of new particle formation from
841   monoterpene oxidation by NOx, Atmos. Chem. Phys., 14, 2789-2804, 10.5194/acp-14-2789-2014, 2014.

842   Worton, D. R., Goldstein, A. H., Farmer, D. K., Docherty, K. S., Jimenez, J. L., Gilman, J. B., Kuster, W. C., de
843   Gouw, J., Williams, B. J., Kreisberg, N. M., Hering, S. V., Bench, G., McKay, M., Kristensen, K., Glasius, M.,
844   Surratt, J. D., and Seinfeld, J. H.: Origins and composition of fine atmospheric carbonaceous aerosol in the Sierra
845   Nevada Mountains, California, Atmos. Chem. Phys., 11, 10219-10241, 10.5194/acp-11-10219-2011, 2011.

846   Wu, Z. J., Poulain, L., Henning, S., Dieckmann, K., Birmili, W., Merkel, M., van Pinxteren, D., Spindler, G.,
847   Muller, K., Stratmann, F., Herrmann, H., and Wiedensohler, A.: Relating particle hygroscopicity and CCN
848   activity to chemical composition during the HCCT-2010 field campaign, Atmos. Chem. Phys., 13, 7983-7996,
849   10.5194/acp-13-7983-2013, 2013.

850   Xu, L., Guo, H. Y., Boyd, C. M., Klein, M., Bougiatioti, A., Cerully, K. M., Hite, J. R., Isaacman-VanWertz, G.,
851   Kreisberg, N. M., Knote, C., Olson, K., Koss, A., Goldstein, A. H., Hering, S. V., de Gouw, J., Baumann, K.,
852   Lee, S. H., Nenes, A., Weber, R. J., and Ng, N. L.: Effects of anthropogenic emissions on aerosol formation from
853   isoprene and monoterpenes in the southeastern United States, Proc. Nat. Acad. Sci. U.S.A., 112, 37-42,
854   10.1073/pnas.1417609112, 2015a.

855   Xu, L., Suresh, S., Guo, H., Weber, R. J., and Ng, N. L.: Aerosol characterization over the southeastern United
856   States using high-resolution aerosol mass spectrometry: spatial and seasonal variation of aerosol composition and
857   sources with a focus on organic nitrates, Atmos. Chem. Phys., 15, 7307-7336, 10.5194/acp-15-7307-2015, 2015b.

858   Ye, P. L., Ding, X., Hakala, J., Hofbauer, V., Robinson, E. S., and Donahue, N. M.: Vapor wall loss of semi-
859   volatile organic compounds in a Teflon chamber, Aerosol Sci. Technol., 50, 822-834,
860   10.1080/02786826.2016.1195905, 2016.

861   Yeung, M. C., Lee, B. P., Li, Y. J., and Chan, C. K.: Simultaneous HTDMA and HR-ToF-AMS measurements at
862   the HKUST Supersite in Hong Kong in 2011, J. Geophys. Res.-Atmos., 119, 9864-9883, 10.1002/2013jd021146,
863   2014.

864   Zhang, J. Y., Hartz, K. E. H., Pandis, S. N., and Donahue, N. M.: Secondary organic aerosol formation from
865   limonene ozonolysis: Homogeneous and heterogeneous influences as a function of NOx, J. Phys. Chem. A 110,
866   11053-11063, 10.1021/jp062836f, 2006.

867   Zhang, Q., Jimenez, J. L., Canagaratna, M. R., Ulbrich, I. M., Ng, N. L., Worsnop, D. R., and Sun, Y. L.:
868   Understanding atmospheric organic aerosols via factor analysis of aerosol mass spectrometry: a review, Anal.
869   Bioanal. Chem., 401, 3045-3067, 10.1007/s00216-011-5355-y, 2011.

870   Zhang, R. Y., Khalizov, A., Wang, L., Hu, M., and Xu, W.: Nucleation and Growth of Nanoparticles in the
871   Atmosphere, Chem. Rev., 112, 1957-2011, 10.1021/cr2001756, 2012.

872   Zhang, S. H., Shaw, M., Seinfeld, J. H., and Flagan, R. C.: Photochemical aerosol formation from alpha-pinene-
873   and beta-pinene, J. Geophys. Res.-Atmos., 97, 20717-20729, 1992.

874   Zhang, X., Cappa, C. D., Jathar, S. H., McVay, R. C., Ensberg, J. J., Kleeman, M. J., and Seinfeld, J. H.:
875   Influence of vapor wall loss in laboratory chambers on yields of secondary organic aerosol, Proc. Nat. Acad. Sci.
876   U.S.A., 111, 5802-5807, 10.1073/pnas.1404727111, 2014.

877   Zhang, X., Schwantes, R. H., McVay, R. C., Lignell, H., Coggon, M. M., Flagan, R. C., and Seinfeld, J. H.:
878   Vapor wall deposition in Teflon chambers, Atmos. Chem. Phys., 15, 4197-4214, 10.5194/acp-15-4197-2015,
879   2015.

880   Zhao, D. F., Buchholz, A., Kortner, B., Schlag, P., Rubach, F., Kiendler-Scharr, A., Tillmann, R., Wahner, A.,
881   Flores, J. M., Rudich, Y., Watne, Å. K., Hallquist, M., Wildt, J., and Mentel, T. F.: Size-dependent
882   hygroscopicity parameter (κ) and chemical composition of secondary organic cloud condensation nuclei,
883   Geophys. Res. Lett., 42, 10920-10928, 10.1002/2015gl066497, 2015a.

884   Zhao, D. F., Kaminski, M., Schlag, P., Fuchs, H., Acir, I. H., Bohn, B., Häseler, R., Kiendler-Scharr, A., Rohrer,
885   F., Tillmann, R., Wang, M. J., Wegener, R., Wildt, J., Wahner, A., and Mentel, T. F.: Secondary organic aerosol
886   formation from hydroxyl radical oxidation and ozonolysis of monoterpenes, Atmos. Chem. Phys., 15, 991-1012,
887   10.5194/acp-15-991-2015, 2015b.

888   Zhao, D. F., Buchholz, A., Kortner, B., Schlag, P., Rubach, F., Fuchs, H., Kiendler-Scharr, A., Tillmann, R.,
889   Wahner, A., Watne, Å. K., Hallquist, M., Flores, J. M., Rudich, Y., Kristensen, K., Hansen, A. M. K., Glasius,
890   M., Kourtchev, I., Kalberer, M., and Mentel, T. F.: Cloud condensation nuclei activity, droplet growth kinetics,
891   and hygroscopicity of biogenic and anthropogenic secondary organic aerosol (SOA), Atmos. Chem. Phys., 16,
892   1105-1121, 10.5194/acp-16-1105-2016, 2016.

893   Ziemann, P. J., and Atkinson, R.: Kinetics, products, and mechanisms of secondary organic aerosol formation,
894   Chem. Soc. Rev., 41, 6582-6605, 10.1039/c2cs35122f, 2012.

895

896

Table 1 Overview of the experiments in this study

Precursor	SO_2	NO_x	NO (ppb)	SO_2 (ppb)
α-pinene	Low SO_2	Low NO_x	0.05-0.2	<0.05
		High NO_x	~20	<0.05
(~20 ppb)	High SO_2	Low NO_x	0.05-0.2	~15
		High NO_x	~20	~15
Limonene	Low SO_2	Low NO_x	0.05-0.2	<0.05
		High NO_x	~20	<0.05
(~7 ppb)	High SO_2	Low NO_x	0.05-0.2	~15
		High NO_x	~20	~15
	Moderate SO_2	High NO_x	~20	~2

899

900 (a) (b)
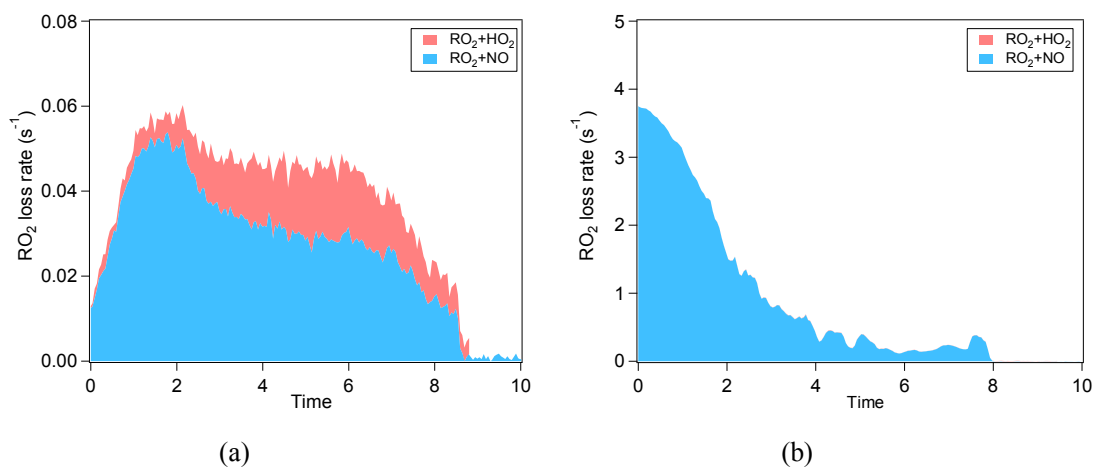
901 Figure 1. Typical loss rate of RO_2 by RO_2+NO and RO_2+HO_2 in the low NO_x (a) and the high NO_x (b) conditions

902 of this study. The experiments at low SO_2 are shown. The RO_2+HO_2 rate is stacked on the RO_2+NO rate. Note

903 the different scales for RO_2 loss rate in panel a and b. In panel b, the contribution of RO_2+HO_2 is very low and
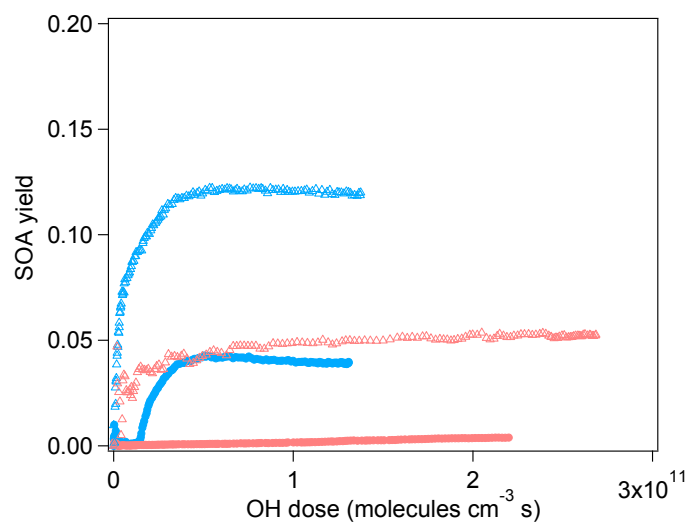
904 barely noticeable.

905
906   (a)   (b)
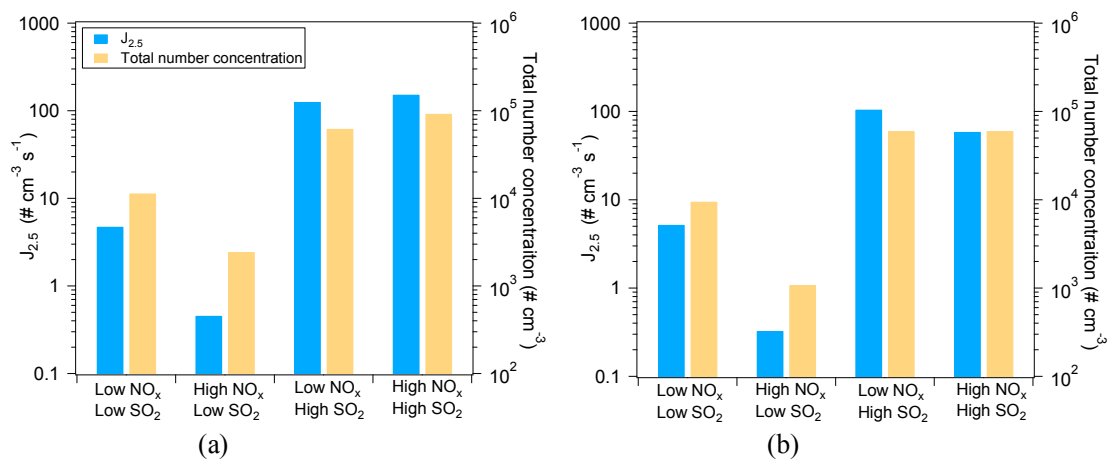
907 Figure 2. Nucleation rates ($J_{2.5}$) and maximum total particle number concentrations under different NO_x and SO_2

908 conditions for the SOA from α-pinene oxidation (a) and from limonene oxidation (b).

909

910

(a)

911
912
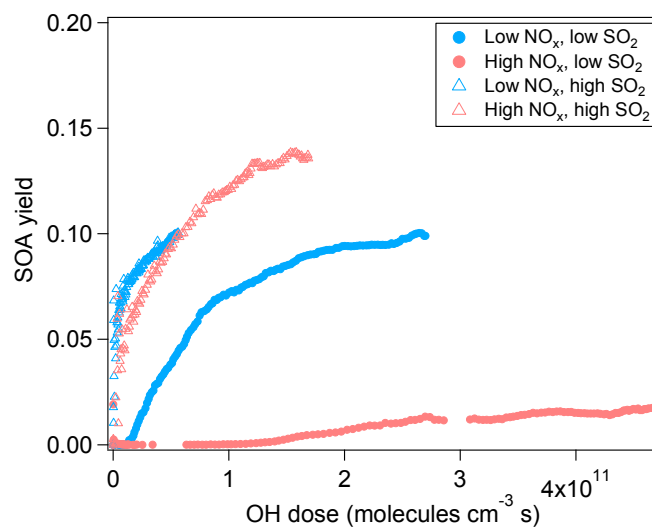
913
914   (b)
915   Figure 3. SOA yield of the photooxidation of α-pinene (a) and limonene (b) in different NO_x and SO_2 conditions.

916

917
918 (a)   (b)
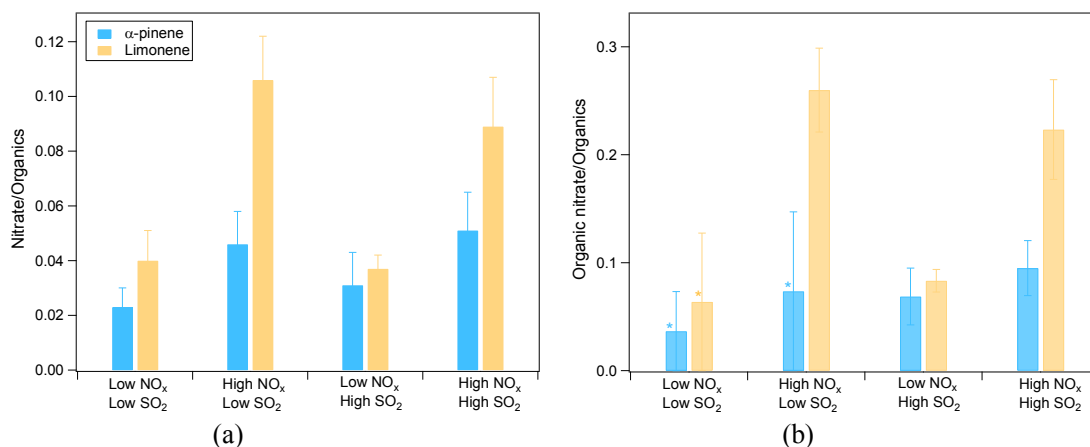
919 Figure 4. (a) The ratio of nitrate mass concentration to organics mass in different NO_x and SO_2 conditions. The

920 average ratios of nitrate to organics during the reaction are shown and error bars indicate the standard deviations.

921 (b) The fraction of organic nitrate to total organics in different NO_x and SO_2 conditions calculated using a

922 molecular weight of 200 g/mol for organic nitrate. The average fractions during the reaction are shown and error

923 bars indicate the standard deviations. In panel b, * indicate the experiments where the ratios of NO_2^+ to NO^+ were

924 too noisy to derive a reliable fraction of organic nitrate. For these experiments, 50% of total nitrate was assumed

925 to be organic nitrate and the error bars show the range when 0 to 100% of nitrate are assumed to be organic

926 nitrate.
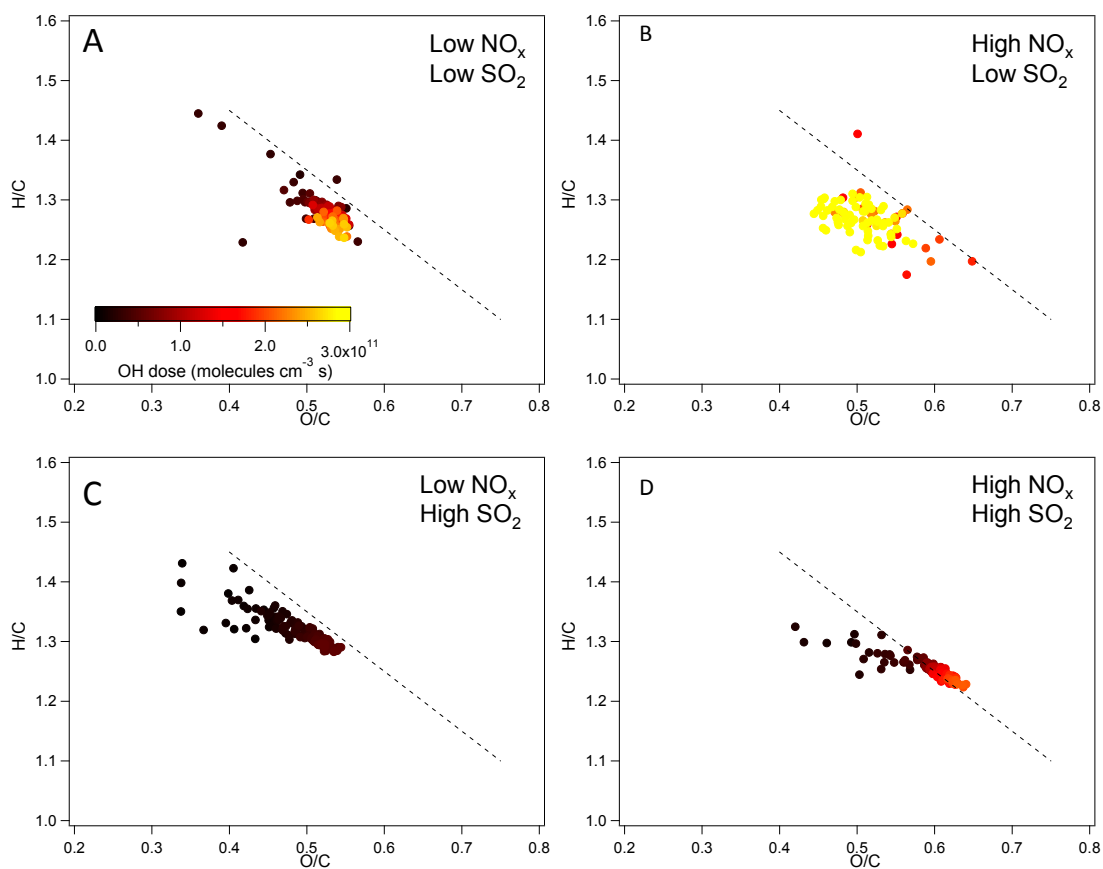
Figure 5. H/C and O/C ratio of SOA from photooxidation of α-pinene in different NOx and SO2 conditions. A: low NOx, low SO2, B: high NOx, low SO2, C: low NOx, high SO2, D: high NOx, high SO2. The black dashed line corresponds to the slope of -1.
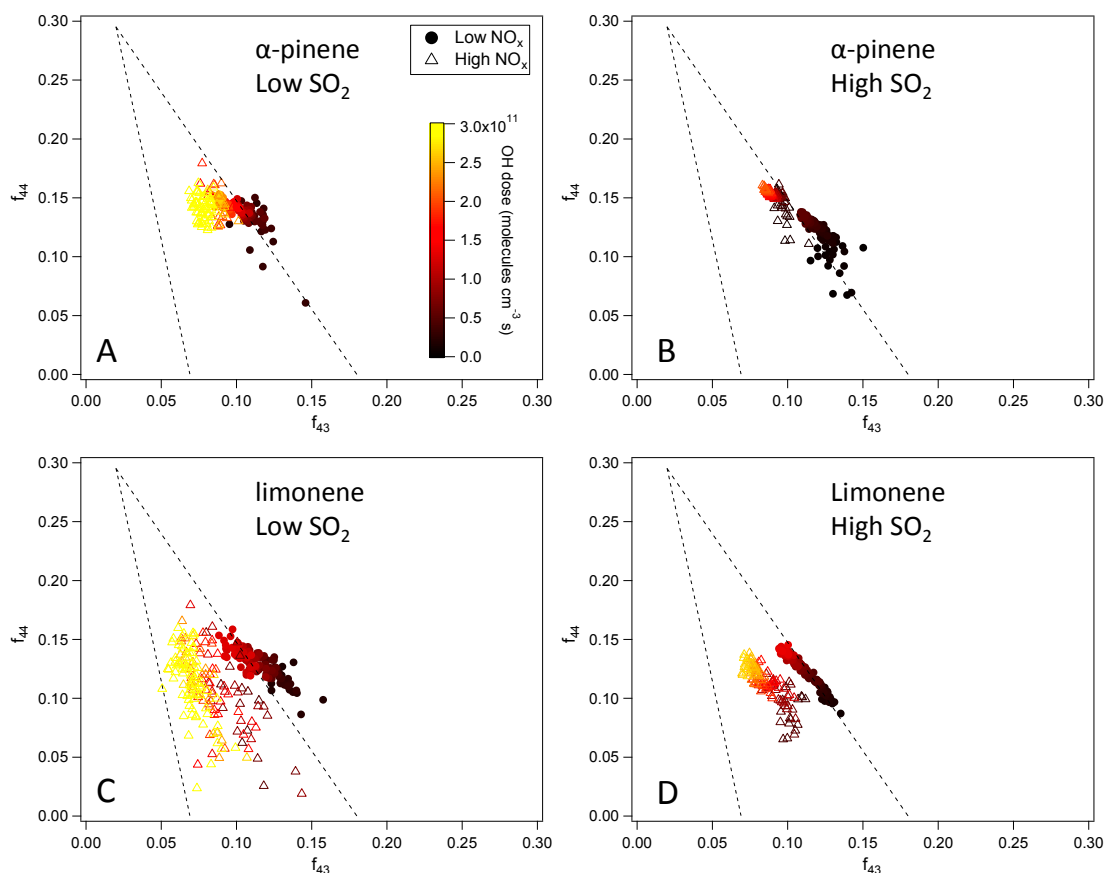
Figure 6. f_{44} and f_{43} of SOA from the photooxidation of α-pinene and limonene in different NO_x and SO_2 conditions. A: α-pinene, low SO_2, B: α-pinene, high SO_2, C: limonene, low SO_2, D: limonene, high SO_2. Note that in the low SO_2, high NO_x condition (panel C), the AMS signal of SOA from limonene oxidation was too low to derive reliable information due to the low particle mass concentration and small particle size. Therefore, the data for high NO_x in panel C show an experiment with moderate SO_2 (2 ppb) and high NO_x instead.

938
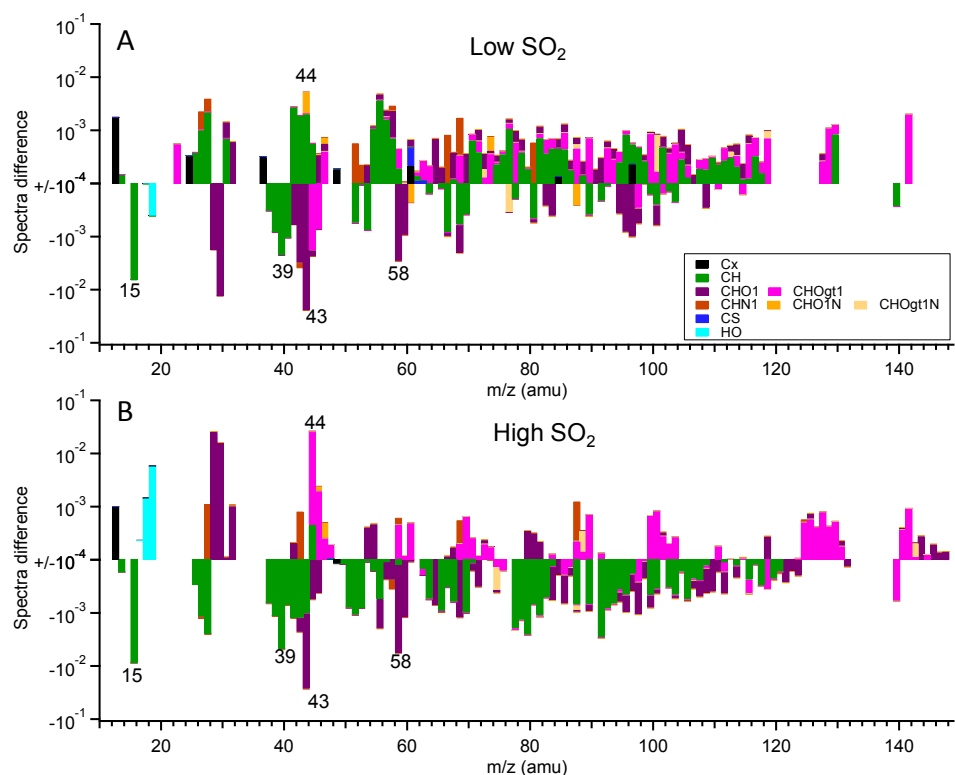939 Figure 7. The difference in the mass spectra of organics of SOA from α-pinene photooxidation between high NO_x
940 and low NO_x conditions (high NO_x-low NO_x). SOA was formed at low SO_2 (a) and high SO_2 (b). The different
941 chemical family of high resolution mass peaks are stacked at each unit mass *m/z* ("gt1" means greater than 1).
942 The mass spectra were normalized to the total organic signals. Note the log scale of y-axis and only the data with
943 absolute values large than 10^{-4} are shown.
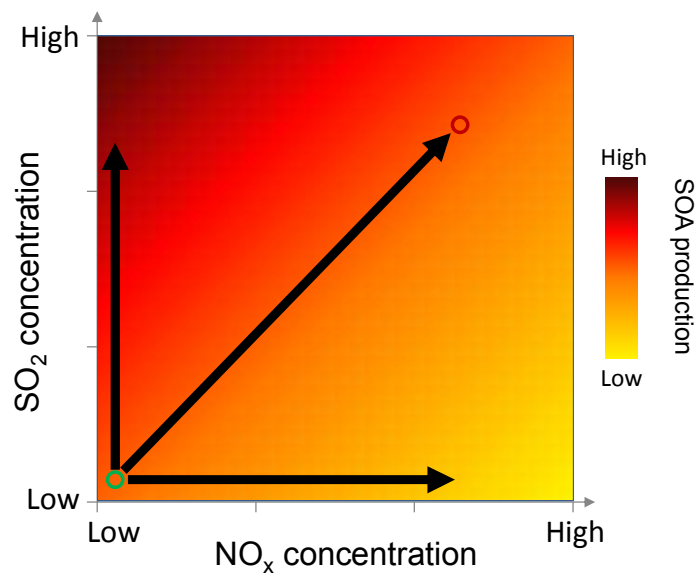
944

945   Figure 8. Conceptual schematic showing how NO_x and SO_2 concentrations affect biogenic SOA mass production.

946   The darker colors indicate higher SOA production. The circle on the bottom left corner indicates biogenic cases

947   and the circle on the right top corner indicates the anthropogenic cases. And the horizontal and vertical arrows

948   indicate the effect of NO_x and SO_2 alone. The overall effects on SOA production depend on specific NO_x, SO_2

949   concentrations and VOC concentrations and speciation.